iScience

Article

Multiomics reveal biomolecular shifts and ER stress in sleep-restricted women affecting NSC functions

Graphical abstract

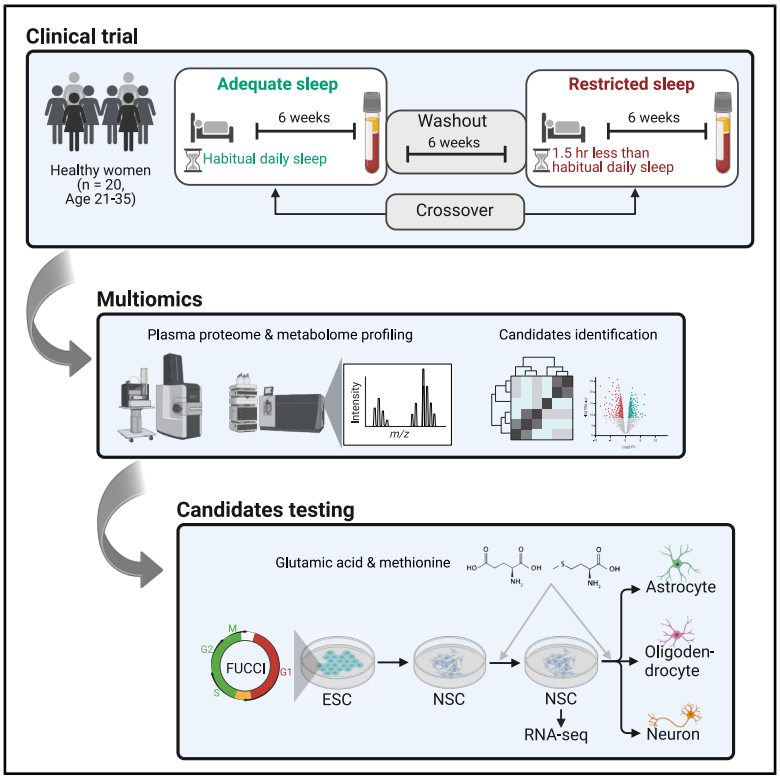

Highlights

- Restricted sleep (RS) drastically alters metabolomic and proteomic profiles
- RS increases circulating amino acids and ER stress-related proteins
- RS-enriched metabolites affect hNSC proliferation, cell cycle, and differentiation
- Stemness loss and stress rise in treated hNSCs converge at HSPA8-ATF ER stress

Authors

Vikas Malik, Xin Huang, Hongwei Zhou, ..., Donald W. Landry, Sanja Jelic, Jianlong Wang

Correspondence

jw3925@cumc.columbia.edu

In brief

Neuroscience; Stem cells research; Omics

Malik et al., 2025, iScience *28*, 112510
May 16, 2025
https://doi.org/10.1016/j.isci.2025.112510

CellPress

iScience

CellPress
OPEN ACCESS

Article

Multiomics reveal biomolecular shifts and ER stress in sleep-restricted women affecting NSC functions

Vikas Malik,[1] Xin Huang,[1] Hongwei Zhou,[1] Rebecca Bojar,[2] Rajesh Kumar Soni,[3] Donald W. Landry,[4] Sanja Jelic,[5] and Jianlong Wang[1,6,*]

[1]Department of Medicine, Columbia Center for Human Development and Stem Cell Therapies, Columbia Stem Cell Initiative, Herbert Irving Comprehensive Cancer Center, Columbia University Irving Medical Center, New York, NY 10032, USA

[2]Barnard College, Columbia University, New York, NY 10027, USA

[3]Proteomics and Macromolecular Crystallography Shared Resource, Herbert Irving Comprehensive Cancer Center, Columbia University Irving Medical Center, New York, NY 10032, USA

[4]Division of Nephrology, Department of Medicine, Columbia University Vagelos College of Physicians and Surgeons, New York-Presbyterian/Columbia University Irving Medical Center, New York, NY 10032, USA

[5]Division of Pulmonary, Allergy, and Critical Care Medicine, Columbia University Vagelos College of Physicians and Surgeons, New York, NY 10032, USA

[6]Lead contact

*Correspondence: jw3925@cumc.columbia.edu

https://doi.org/10.1016/j.isci.2025.112510

SUMMARY

Adequate sleep (AS) is vital for physiological functions, yet a third of US adults sleep less than recommended. While circadian rhythms regulate adult stem cell functions, the impact of insufficient sleep remains unclear. We previously completed a clinical trial in healthy women in a randomized crossover design of 6-week periods with AS or mildly restricted sleep (RS; 1.5 h less). Here, we performed metabolomic and proteomic profiling of plasma samples. RS induced a stress-like state, highlighted by ER stress, heat shock, ubiquitination proteins, and amino acid biosynthesis. RS was strongly linked to disrupted neural development. Treating neural stem cells (NSCs) derived from human embryonic stem cells with RS-enriched metabolites disrupted G1 cell cycle phase and impaired differentiation into neurons, astrocytes, and oligodendrocytes. Our findings reveal how mild RS, mimicking "real-life" conditions, disrupts NSC divisions and differentiation, highlighting the critical role of sleep in adult stem cell regulation and neural development.

INTRODUCTION

Despite sleep being an essential and non-negotiable bodily function, humans are the only species that voluntarily curtail it. Adequate sleep (AS) of 7–9 h/night[1,2] is necessary for most adults to achieve optimal daytime performance and well-being. Chronic insufficient sleep is associated with impaired mental, cognitive, and behavioral health, an increased risk of metabolic, cardiovascular, and immunological diseases,[3] and a shortened life span.[4–6]

Longevity regulation is intricately linked to circadian rhythm and stem cell pluripotency network.[7,8] AS promotes a suitable microenvironment for stem cells to proliferate, migrate, and differentiate, thus maintaining homeostasis. Circadian rhythm genes directly control various stem cells, including germline stem cells in drosophila,[9] bone marrow mesenchymal,[10] embryonic,[11] epidermal,[12,13] and neural[14,15] stem cells in the mouse. Sleep interruption modifies hematopoietic stem cell epigenome and, thus, hematopoiesis in humans and mice.[16–18] In mice, sleep deprivation also leads to reduced hematopoietic stem cell transplantation efficiency[19] and hyperproliferation of corneal epithelial progenitor cells, followed by scarcity after long-term sleep deprivation.[20] Patients with obstructive sleep apnea, characterized by sleep fragmentation and deprivation, have a 3- to 4-fold reduction in bone marrow-derived endothelial progenitor cells compared to healthy individuals.[21,22] Similarly, sleep-regulated molecules, such as hormones (e.g., melatonin, serotonin, vasopressin, and growth hormone),[23] lactate,[24] and glutamine[25,26] are reported to control stem cell homeostasis. However, the biomarkers of sleep deprivation, especially in humans, are not clearly defined.

Several metabolomics[27–30] and proteomics[31–34] studies have begun identifying key biomarkers of restricted sleep (RS) in mice. However, such studies of metabolomics[30,35–37] and proteomics[38] in humans are limited, and integrated multiomics approaches have only been applied in rodents.[39,40] Limitations of existing human studies include the use of severe, short-term sleep restriction interventions (1–10 days) that may not reflect typical sleep patterns, small sample sizes ($n < 10$) (reviewed by ref. 41), and the lack of sufficiently long, objectively monitored, randomized sleep restriction intervention, as well as limited experimental validations on the consequences of sleep

restriction. Consequently, the direct effects of mild and chronic sleep restriction, a sleep pattern practiced by a third of the adult population in the United States, on adult stem cells remain undefined. Thus, our understanding of the causal relationship between sleep restriction and stem cell homeostasis remains obscure.

Sleep requirements may differ for different sexes. For example, women may need longer sleep than men for optimal daytime functioning.[42,43] Women are more likely to suffer from anxiety[44] and depression,[45] which may also be related to a 40% greater prevalence of insomnia than men.[46–48] Furthermore, women have greater pro-inflammatory responses and a more pronounced cardiovascular risk associated with insufficient sleep.[49–52] Since sleep restriction affects women differently and more severely than men, we previously conducted a clinical trial focusing on women (ClinicalTrials.gov NCT02835261) and discovered that sleep restriction increases endothelial inflammation, resulting in endothelial dysfunction in healthy women.[53,54] Here, we aimed to identify sleep restriction biomarkers and understand their effects on restorative and regenerative functions in women.

Using a randomized crossover design and metabolomic and proteomic profiling of plasma collected from women after 6 weeks of objectively monitored AS or RS, the longest trial to date, we identified key metabolites and proteins that are altered with sleep restriction. Specifically, we found that essential biomolecules, i.e., glutamic acid and methionine, accumulated in sleep-restricted women's plasma and could negatively impact neural stem cell (NSC) homeostasis and differentiation potential when tested *in vitro*. We also identified endoplasmic reticulum (ER) stress response pathway activation as the highly conserved adaptive protection response to sleep restriction in women. These findings suggest that chronic, insufficient sleep modifies stress response pathways, inducing changes in NSC homeostasis and a potentially increasing risk for neurodegenerative diseases in the long term.

RESULTS

Plasma metabolomic profiles identified candidate metabolites as potential biomarkers for adequate versus restricted sleep

We used blood plasma samples collected from healthy women (n = 20; mean ± SD: age 27 ± 4 years; BMI 25.2 ± 2.7 kg/m^2; 50% racial and ethnic minorities, Table S1) who participated in our sleep restriction clinical trial (ClinicalTrials.gov NCT0283 5261). After completing a 2-week actigraphy screening to establish that their habitual sleep duration is adequate (7–9 h daily), healthy women were randomized to a 6-week AS phase (sleep duration between regular bedtime and wake-time determined during actigraphy screening) or a 6-week RS phase (delaying bedtime by 1.5 h and keeping wake-up time constant) followed by a 6-week washout period and crossover to the alternate sleep phase. Sleep duration was monitored objectively by actigraphy during both study phases (Figure 1A; see STAR Methods for details). Using a combination of flow injection analysis-tandem mass spectrometry (FIA-MS/MS; for lipids and hexoses) and liquid chromatography-tandem mass spectrometry (LC-MS/MS; for small molecules), we studied 630 biochemicals representing 23 classes, including amino acids, bile acids, fatty acids, acylcarnitines, cholesterol esters, di- and tri-glycerides by targeted metabolomics (Figure S1A; Table S2). Partial least squares-discriminant analysis (PLS-DA) of all data showed a clear variation in the metabolomes of AS and RS samples (Figure 1B), where lipids, amino acids, and bile acids were among the main contributing factors to these differences (Figure S1B). We also performed fold-change analysis and under RS conditions identified 97 upregulated and 21 downregulated (or upregulated in AS) metabolites (Figure 1C; Table S3), consisting of triglycerols, unsaturated fatty acids, amino acids, and fatty acyl carnitines among a range of classes (Figure S1C).

Next, we combined the results of both the PLS-DA (Figure 1B) and fold-change (Figure 1C) analyses to shortlist the top 5 candidates based on the PLS-DA VIP (variable importance in projection) score and another top 5 based on fold-change (t-test) (Figures 1D and S1D). We identified TG(20:1_32:3), a triglyceride, and DG(16:0_18:1), a diglyceride, as the top candidates for AS in both PLS-DA VIP and t-test-based analyses. In contrast, the circulating levels of arachidonic acid, fatty acids (FA(18:1) and FA(20:2)), amino acids (glutamic acid and methionine), and LysoPC a C20:3 were increased under RS conditions (Figures 1C and 1D). In summary, our study identified candidate metabolites as potential biomarkers enriched or depleted after RS.

Plasma proteomic profiles identified protein folding and stress signaling pathways after mild sleep restriction in women

To better understand the molecular consequences of sleep restriction, we performed proteomics in parallel on the same plasma samples (Figure S2A). Of the 1001 identified proteins (Table S4), 253 were upregulated and 113 were downregulated (absolute difference fold change 0.1) in RS compared to AS (Figure 2A; Table S5). Among the 253 enriched proteins under RS conditions, many of them significantly (p-value <1.0e-16) interact with one another (Figure S2B). Many were involved in actin cytoskeleton organization (n = 16), protein folding/stability (n = 10), stress response (n = 20), and G2/M cell cycle checkpoint (n = 4), among other biological processes and Reactome pathways (Figure S2B; Table S6). Proteins associated with the above four gene ontology (GO) terms were expressed significantly higher in RS than in AS conditions (Figure S2C).

A comparative GO analysis of differentially expressed proteins showed enrichment of terms such as "formation of cornified envelope" and "adaptive immune response" in AS compared to RS (Figure 2B). In contrast, GO terms such as "protein stability (polymerization, folding, polyubiquitination)," "stress induced heat shock proteins," and "signaling pathways (neurotrophin, FAS ligand, and IκB/NF-κB)" were enriched in RS conditions, suggesting that sleep restriction led to the activation of stress response (Figure 2B). Furthermore, we have recently shown that the nuclear NF-κB levels were indeed greater in the endothelial cells obtained from women after RS compared to AS,[54] thus corroborating our proteomics findings. Notably, interacting proteins (Figure S2B), including heat shock proteins (e.g., HSPA8, HSPA1A/B), ubiquitination proteins (e.g., UBE2V1), cell cycle

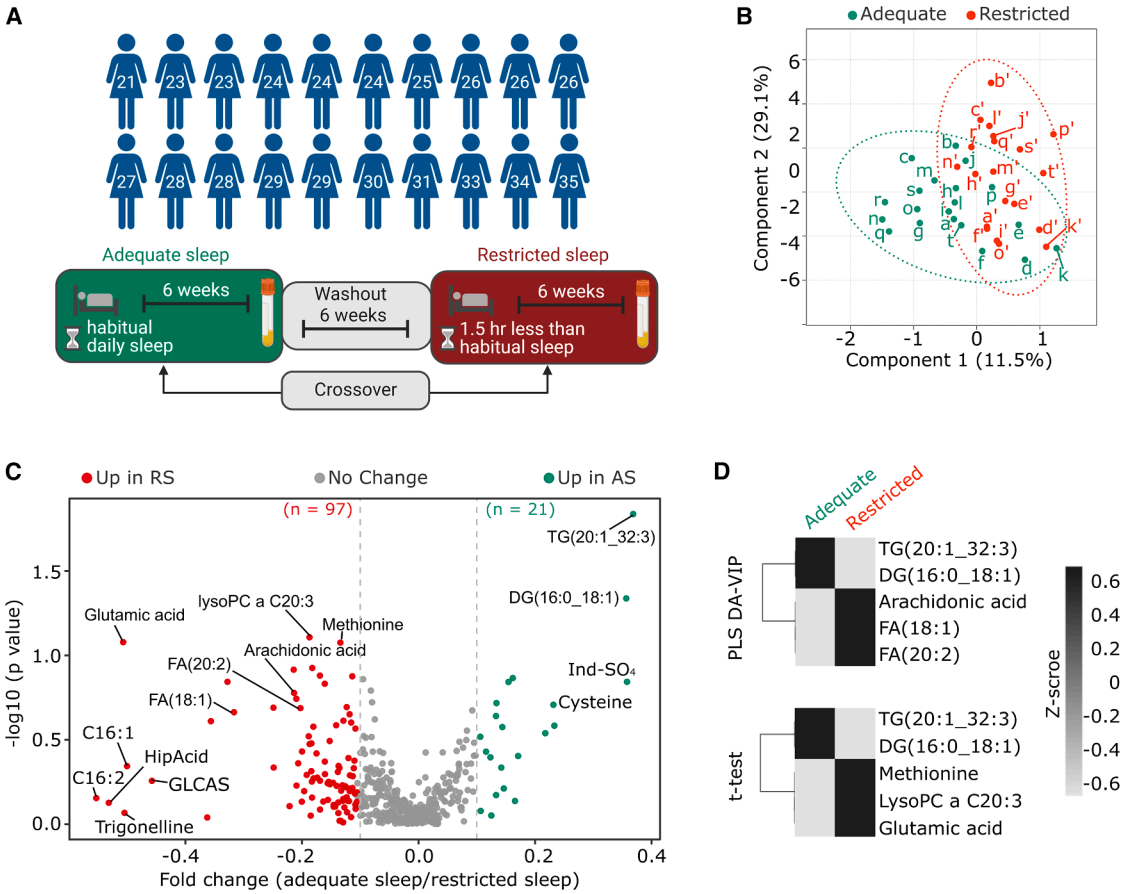

Figure 1. The metabolic profile separated sleep restriction from adequate sleep samples

(A) Schematic representation of sleep restriction study (ClinicalTrials.gov NCT02835261[53,54]). Plasma samples from women (n = 20) between 21 and 35 years of age were selected for multiomics in the current study. The age of each participant is indicated. Plasma samples were obtained after both adequate and restricted sleep phases. See STAR Methods and Table S1 for participants' details.

(B) PLS-DA plot showing the separation of adequate (green) from restricted sleep (red) conditions. Each point represents one woman, and the dotted ellipses represent 95% confidence intervals. The samples are from the crossover study and, therefore, are paired. Alphabets in green represent data from individuals who received adequate sleep, while the corresponding alphabets with a dash in red represent data from the same woman after experiencing restricted sleep. See also Table S2.

(C) Volcano plots showing the distribution of fold changes in metabolite concentrations between adequate and restricted sleep conditions with selected candidates highlighted. The vertical dashed lines represent the absolute $\log_2$ fold change (>0.1) cut-off. The numbers of differentially enriched metabolites are indicated at the top, and details are provided in Table S3.

(D) Heatmaps showing the top 5 regulated metabolites based on either VIP score from PLS-DA (upper panel) or t-test (lower panel) analyses in adequate and restricted sleep conditions. See also Figure S1.

regulator (YWHAB), and cytoskeleton proteins (e.g., ACTB, ACTBL2), were significantly upregulated in RS (Figures 2C and 2D).

The enrichment of the "adaptive immune response" under AS conditions (Figure 2B) aligns well with previous reports suggesting the beneficial roles of AS before and after vaccination in generating higher antibody titers,[61] as well as a better secondary antibody response[62] and a higher fraction of interferon-γ (IFN-γ)-positive immune cells.[63] Previous work using proteomics in mice also suggests that I-κB/NF-κB,[64] protein folding,[32,33,65] and stress response[32,33,38] increase during sleep restriction, highlighting species-level conservation of these response pathways to sleep restriction. Heat shock proteins, and HSPA8 in particular, have been reported to increase after sleep disruption.[31,33,66–68] Together, these results suggest that sleep restriction may lead to the perturbation of cellular immunity, induction of stress responses, protein ubiquitination, and homeostatic imbalance.

The activation of the stress response after sleep restriction is associated with ATF6/ER stress response

To explore the potential molecular mechanism underlying differential protein enrichment in RS versus AS in women, we focused on transcription factors (TFs) due to their prominent roles in gene regulation. The intersection of differentially upregulated proteins under RS conditions (n = 253) with the list of publicly annotated

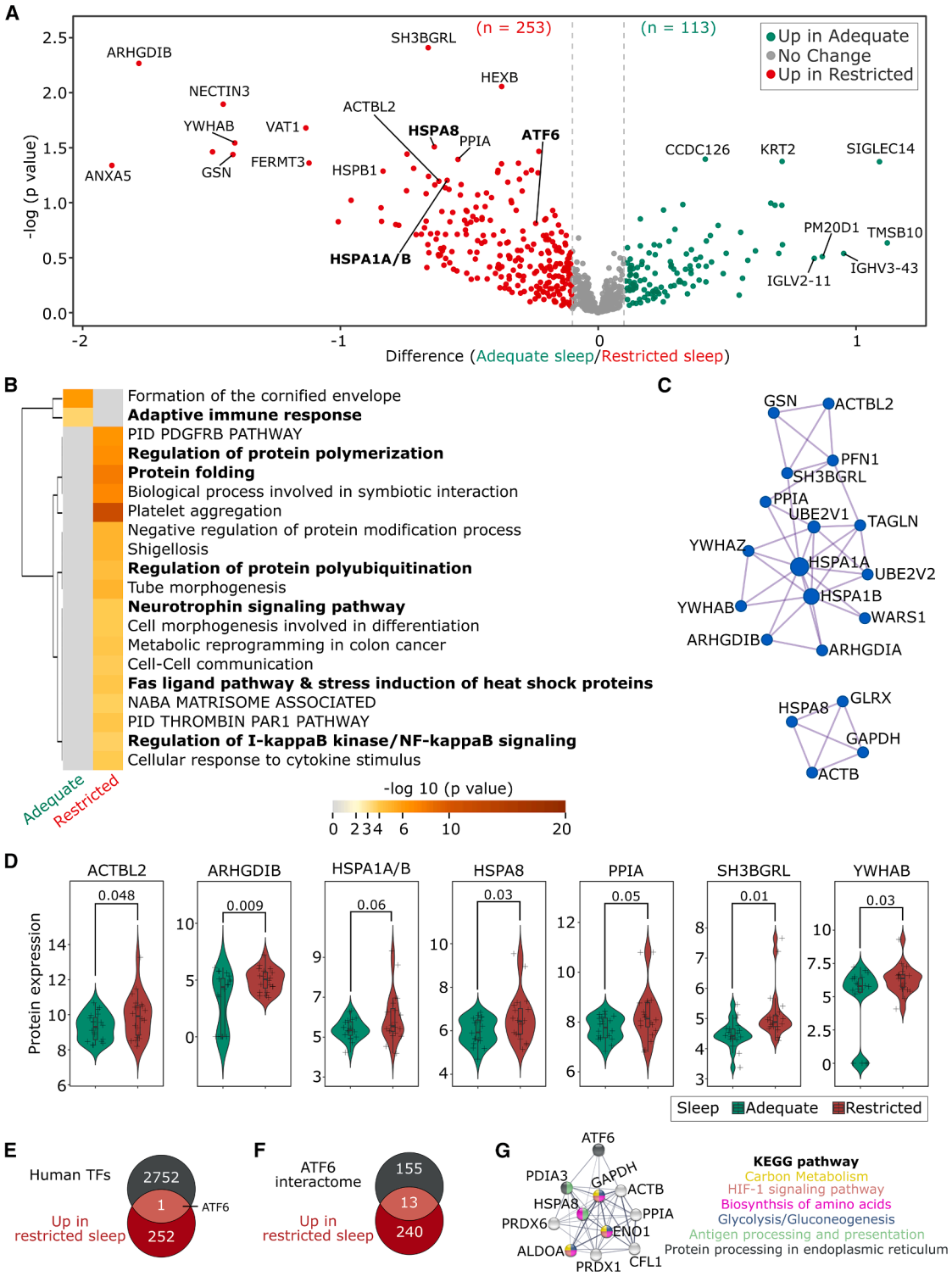

Figure 2. Plasma proteomic profiles identified protein folding and stress signaling pathways associated with sleep-restricted women

(A) Volcano plot of differential protein expression between adequate and restricted sleep conditions using Perseus.[55] The vertical dashed lines represent the absolute difference (>0.1) cut-off, and selected candidates are highlighted. The numbers of differentially enriched proteins are indicated on the top, and details are provided in Tables S4 and S5.

(B) GO analysis of 253 and 113 proteins from (A) using metascape.[56] See also Table S6.

(C) Protein-protein interaction analysis maps drawn using differentially expressed proteins associated with GO terms in (B) with metascape.[56]

(legend continued on next page)

TFs (n = 2765)[57] identified ATF6 as the sole overlapping TF (Figure 2E). ATF6 regulates organogenesis and tissue homeostasis with established roles in protein folding, ER stress sensing, and the activation of stress response pathways to establish a protective cellular state.[69] Notably, ATF6 signaling is also a part of sleep fragmentation-induced ER stress.[70] The prominent enrichment of GO terms involving protein stability and folding upon sleep restriction (Figure 2B) prompted us to test the hypothesis that ATF6 may act as a major regulator of RS-induced proteostasis by transcriptionally activating and/or physically interacting with those factors enriched in sleep-restricted women.

By intersecting previously identified partners of ATF6[58] with proteins upregulated under RS conditions, we identified 13 overlapping proteins (Figure 2F), including ATF6, chaperones (PDIA3 and P4HB), cytoskeleton regulators (ACTB and CFL1), peptidyl-prolyl *cis*-trans isomerase (PPIA), antioxidants (PRDX1/6), glycolytic enzymes (ALDOA, GAPDH, and ENO1), heat shock protein (HSPA8), and immunoglobulin (IGLV1-47) (Figure S2D). ATF6 is a TF that homodimerizes and binds to promoter regions of target genes upon its activation following ER stress sensing.[69] Interestingly, when analyzing publicly available ATF6 ChIP-seq data in HepG2 cells,[58] we found that the promoters of almost all (except IGLV1-47, which was not detected in the RefSeq database) of the above 13 protein-coding genes contain a binding site for ATF6 (Figure S2E), supporting the key role of ATF6 in transcriptional activation of these genes in RS-induced proteostasis. Consistently, ATF6 has been shown to activate PDIA3 in zebrafish[71] and human mesenchymal stem cells[72] by binding directly at the consensus ERSE (ER stress response element) $CCAATN_9CCAC[GA]$[73] motif in the promoter region (Figure S2E). ATF6 binding to its own promoter may suggest autoregulation. ATF6-interacting and target proteins that were upregulated after RS showed a significant protein-protein interaction network (PPI enrichment p-value <1.0e-16) and were associated with KEGG pathway terms such as "carbon metabolism," "HIF-1 signaling pathway," "biosynthesis of amino acids," "glycolysis/gluconeogenesis," "antigen processing and presentation," and "protein processing in the endoplasmic reticulum" (Figure 2G). Together, our data highlight a close-knit stress response circuit activated upon sleep restriction through ATF6 and its downstream pathway.

Derivation of FUCCI-hNSCs as a model system for studying adult stem cell functions after sleep restriction

To better understand the functional interaction between metabolites and proteins after sleep restriction, we performed a joint network analysis using differentially enriched top metabolites (n = 25, absolute fold change >0.2) and proteins (n = 83; absolute difference >0.2, Table S7). We observed "estrogen and neurotrophin signaling pathways," "long-term depression/potentiation," "glutathione metabolism," and "circadian entrainment" among the top 25 enriched GO terms, with "D-glutamine/D-glutamate metabolism" and "glutamatergic/dopaminergic synapse" as additional enriched GO terms (Figure 3A). Corroborating our findings, enrichment of the GO term "long-term potentiation" has been reported in a sleep-restricted rat hypothalamus proteomic study.[65] As numerous top enriched terms are related to the nervous system and more than half of the candidate proteins are expressed in the brain (Figure S3A), we examined how sleep restriction affects adult stem cell homeostasis using a human neural stem cell (hNSC) model.

We used the fluorescent, ubiquitination-based cell cycle indicator (FUCCI) reporter system (Figure 3B), which utilizes two cell cycle-specific proteins with red (CDT1-Kusabira orange 2) and green (Geminin-Azami green 1) fluorescent proteins to visually track different phases of the cell cycle in living cells.[77,78] We converted FUCCI-hESCs (human embryonic stem cells) to FUCCI-hNSCs using defined culture conditions (Figure S3B), which was further confirmed by cell morphology (Figure S3C) and the expression of lineage-specific markers measured by qRT-PCR (Figure S3D). The FUCCI-hESCs underwent morphological changes to become FUCCI-hNSCs within 7 days (passage 0), which showed elongated cells on day 13 (passage 1) compared to the compact, round colony morphology at day 0 (Figure S3C). These NSCs show an immediate shutdown of pluripotency markers (e.g., OCT4 and NANOG) and a gradual increase of NSC markers (e.g., PAX6 and NESTIN) at mRNA levels (Figure S3D). To further characterize these cells, we performed live-cell imaging and FACS analysis. We found that FUCCI-hESCs have only 7.67% cells in the G1 phase and a larger population (39.19%) in the S/G2/M phase of the cell cycle (Figures 3B and 3C). In contrast, hNSCs have a larger population in the G1 phase (27.83%) while only 19.23% in the S/G2/M phases of the cell cycle, coinciding with a slower growth rate of hNSCs than hESCs.[79] Thus, we successfully established the FUCCI reporter hNSCs model system for studying the consequences of molecules accumulated under RS conditions.

Treatment with glutamic acid and methionine alters cell proliferation and cell cycle profiles in hNSCs

To investigate the effects of sleep restriction, we subjected FUCCI-hNSCs to treatment using pooled plasma samples from women in corresponding groups with either AS or RS. The limited availability of plasma samples restricted the treatment to a maximum of 13 days, with plasma supplementation every other day, from which RNA-seq analyses were performed. Compared to untreated FUCCI-hNSCs, we observed transcriptional differences after both adequate (n = 99, $\log_2$ fold change 1 and p-value 0.05) and restricted (n = 129, $\log_2$ fold change 1 and p-value 0.05) sleep plasma treatments (Figure S4A; Table S8). However, comparing AS and RS plasma-treated FUCCI-hNSCs did not reveal significant transcriptional differences after 13 days of

(D) Boxplots of significantly overexpressed protein candidates under sleep restriction conditions from the protein-protein interaction map in (C) under adequate and restricted sleep conditions. The indicated p-values were calculated using the paired t-test (R function t-test).
(E and F) Venn diagram showing the intersection of proteins upregulated under sleep restriction conditions (from Figure 2A) with human TFs[57] (E) and the ATF6 interactome[58] (F).
(G) Using STRING,[59,60] a protein-protein interaction map of overlapping proteins (n = 13) was drawn in the ATF6 interactome and the sleep restriction condition. Non-interacting proteins were removed, and line thickness represents the strength of the data support. See also Figure S2.

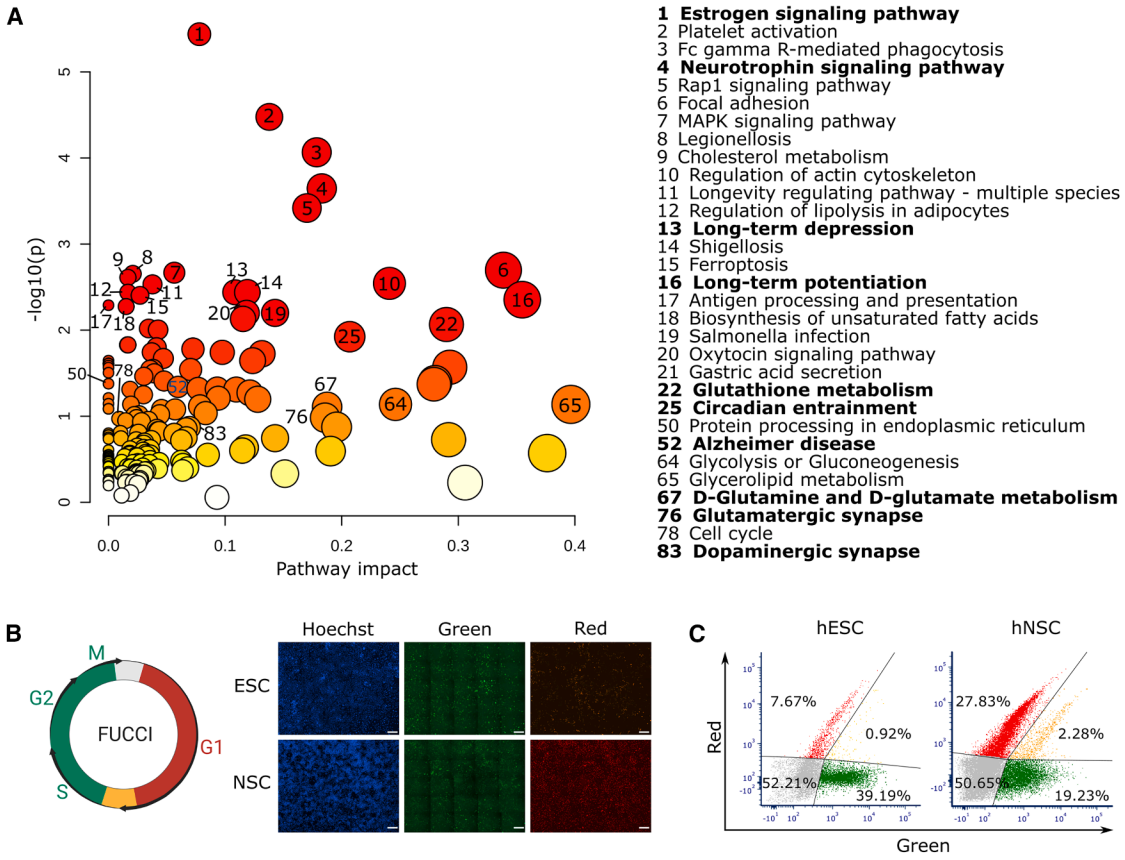

Figure 3. Candidates identified from sleep restriction metabolomics and proteomics are associated with the regulation of the nervous system

(A) Joint network analysis using MetaboAnalyst[74–76] using the top protein (Proteins FC > 0.5 (n = 82) and metabolite FC > 0.2 (n = 25)) candidates (Table S7). The node color is based on its p-value from the pathway enrichment analysis, and the node radius is determined based on their pathway impact values from the pathway topology analysis.

(B) Overview of the FUCCI system based on the fusion of two cell cycle-specific proteins with red (CDT1-Kusabira orange 2) and green (Geminin-Azami green 1) fluorescent proteins, respectively.[77] Representative whole-well live cell scans from a 96-well plate using UV (Hoechst staining), green and red channels for FUCCI-hESCs (top) and FUCCI-hNSCs (bottom) with a 10x objective lens. The scale bar is 0.5 mm.

(C) Flow cytometry analysis of the relative proportion of FUCCI-hESCs and FUCCI-hNSCs in each cell cycle phase. Percentages are indicated in each gate. See also Figure S3.

treatment (Figure S4A). Consequently, we used a more targeted approach by shortlisting amino acids (glutamic acid and methionine) as primary metabolite candidates among those enriched after RS (Figures 1C and 1D), which allowed for a longer treatment of FUCCI-hNSCs corresponding with women's RS exposure in our study. These metabolites were selected for the following reasons: (1) Multiomics GO terms are associated with the nervous system and glutamic acid-related biology (Figure 3A); (2) GO terms associated with the ATF6 interactome proteins upregulated upon RS were related to "amino acid biosynthesis" (Figure 2G), and it is reported that ER stress is associated with amino acid biosynthesis[80]; (3) amino acids can cross the blood-brain barrier,[81] making them feasible candidates in RS plasma samples to affect NSC functions in the brain; (4) glutamate, the ionized form of glutamic acid, was reported to have high expression during the wake phase and reduced expression during the sleep cycle.[82,83] In a metabolomics study, methionine was reported to be enriched after sleep restriction[35]; and, finally, (5) amino acids are readily available commercially and amenable to drug development. However, how these two candidate metabolites control NSC homeostasis has not been studied.

Guided by the circulating maximum plasma concentration of glutamic acid (178 μM) and methionine (33.7 μM) observed in human plasma samples (Table S2), we first treated FUCCI-hNSCs for four days with glutamic acid (200 μM) and methionine (35 μM), respectively, which did not cause any noticeable death of FUCCI-hNSCs but instead showed a higher cell density than untreated cells (Figure S4B). Upon counting cells according to Hoechst staining using live cell imaging (Figure 4A), we found that treatment with glutamic acid and methionine significantly increased cell count compared to the untreated hNSCs (Figure 4B), suggesting increased self-renewal of treated hNSCs. However, the sleep restriction in women was prolonged in our study. Thus, we treated these cells for 30 days with fresh supplementation of metabolites every other day (Figure 4C). Further FACS analysis revealed a massive decrease in the red

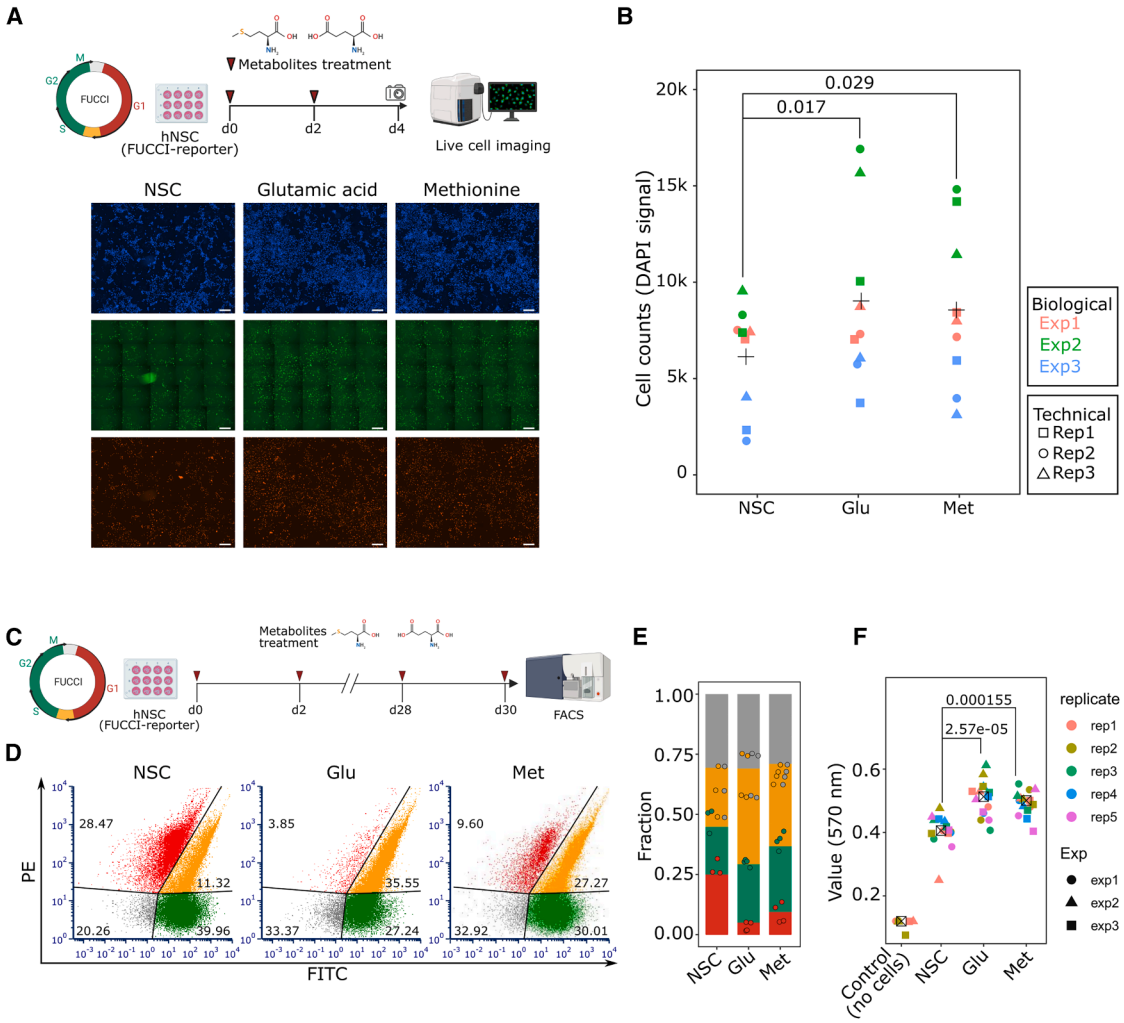

Figure 4. Long-term glutamic acid and methionine treatments cause cell cycle (G1-phase) dysregulation in FUCCI-hNSCs

(A and B) (A) Schematic representation for the short-term (four-days) treatment of FUCCI-hNSCs with metabolites (glutamic acid-200 μM or methionine-35 μM); representative whole-well live cell scans (lower panel) from a 96-well plate using UV (Hoechst staining), green and red channels with a 10x objective lens and (B) cell counts based on Hoechst staining signal (in the right panel) using CellProfiler.[84] Each data point (n = 3 biological replicates, each with n = 3, technical replicates) is shown with the mean as a plus symbol; indicated p-values were calculated using Student's t test. The scale bar is 0.5 mm.

(C) Schematic representation for long-term (thirty days) treatment of FUCCI-hNSCs with metabolites (glutamic acid-200 μM or methionine-35 μM); see STAR Methods for details.

(D and E) Flow cytometry (D) analysis and (E) quantification of the relative proportion of control and treated FUCCI-hNSCs in each cell-cycle phase. Percentages are indicated in each gate. Each data point (n = 3 or 4 biological replicates) is shown in E.

(F) FUCCI-hNSCs proliferation rate determined using an MTT-based assay after a long-term (thirty days) treatment with glutamic acid and methionine. Each data point (n = 3 biological replicates, each with n = 5, technical replicates) is shown with the mean as a square-cross symbol; indicated p-values were calculated using Student's t test. See also Figure S4.

populations (suggestive of a shortened G1 phase) and an increase in yellow populations (suggestive of cells stuck at the G1/S checkpoint) in glutamic acid and methionine treatment conditions compared to the control NSCs (Figures 4D and 4E). Importantly, long-term treatment of hNSCs with glutamic acid and methionine maintained significantly higher proliferation rates than untreated hNSCs (Figure 4F). The G1 phase is the main determinant of stem cell differentiation,[85] and a shortened G1 in NSCs is correlated with inhibited neurogenesis and increased self-renewal proliferation.[86] Together, our results suggest that sleep restriction could compromise neurogenesis in women owing to the dysregulated NSC homeostasis resulting from the impact of accumulated glutamic acid and methionine.

Stemness decline and stress response increase in metabolite-treated hNSCs converge at HSPA8 and ATF-mediated ER stress response

To gain a molecular understanding of the effect of the long-term treatment of glutamic acid and methionine on FUCCI-hNSCs, we performed RNA-seq to scrutinize their transcriptional

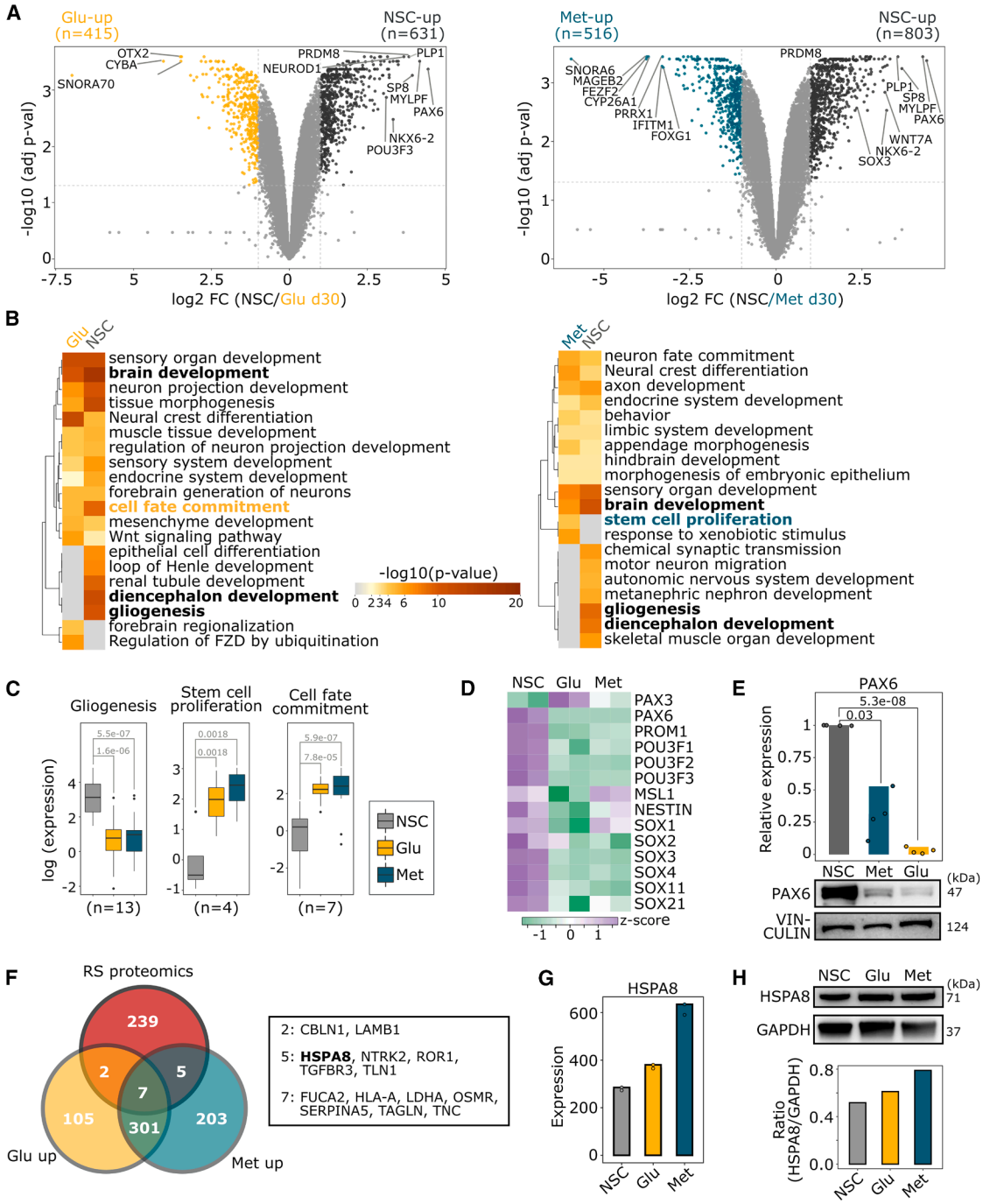

Figure 5. Long-term glutamic acid and methionine treatments reduce stemness and increase stress in hNSCs

(A) Volcano plots of differential gene expression of untreated versus glutamic acid (left panel) or methionine treated (right) with selected candidates highlighted. The horizontal and vertical dashed lines represent the false discovery rate (FDR, 0.05) and $\log_2$ fold change (±0.5) cut-offs, respectively. The numbers of differentially expressed genes are indicated on the top corners, and details are provided in Tables S9 and S10.

(B) GO analysis using metascape[56] for differentially expressed top 100 genes from untreated versus glutamic acid (left) or methionine (right) treated FUCCI-hNSCs.

(C) Boxplots of RNA-seq signals of selected genes associated with indicated GO terms from heat maps in (B). "n" indicates the number of genes associated with each GO term; *p*-values were determined using the Mann–Whitney Wilcoxon test.

(D) Heatmap shows the expression of selected neural stem cell markers for untreated versus glutamic acid or methionine-treated FUCCI-hNSCs. Data are presented as *Z* score normalized counts.

(legend continued on next page)

signatures. Treatments with glutamic acid (415 up and 631 down, $\log_2$ fold change >1 and q-value <0.05) or methionine (516 up and 803 down genes) led to a larger transcriptional difference than untreated FUCCI-hNSCs (Figure 5A; Tables S9 and S10). However, the transcriptional profile was only subtly different between glutamic acid and methionine treatments (25 up and 38 down, Figures S5A and S5B; Table S11), suggesting that long-term exposure to these two metabolites has overlapping effects in hNSCs. Remarkably, the top 100 differentially expressed genes (Figure S5C) from glutamic acid (Glu)- or methionine (Met)-treated versus untreated hNSCs (NSC) are similarly enriched for the GO terms like "brain development," "diencephalon development," and "gliogenesis" (Figure 5B). However, Glu- and Met-treated compared to untreated NSC cells also differ in their enrichment of GO terms "cell fate commitment" and "stem cell proliferation," respectively (Figure 5B). Notably, the expression of gliogenesis-related genes is downregulated. In contrast, the expression of stem cell proliferation- and cell fate commitment-related genes is upregulated in Glu- and Met-treated versus untreated NSCs (Figures 5C, S5C, and S5D). Consistently, both treatments showed a striking downregulation of NSC markers, including PAX, POU, and SOX family members (Figures 5D and 5E), suggesting that NSC stemness is compromised.

Next, upon intersecting the proteins upregulated after sleep restriction in women (Figure 2A) with transcripts upregulated following the two metabolite treatments (Figure 5A), HSPA8 emerged, alongside 13 other candidates, as a pivotal node or convergence point in the signaling pathways influenced by sleep restriction *in vivo* and metabolite effects *in vitro* (Figures 5F, S5E, and S5F). Consistently, both HSPA8 mRNA and protein levels were elevated in glutamic acid- and methionine-treated compared to untreated NSCs (Figures 5G and 5H). HSPA8 is associated with ER stress response,[87] which acts through three molecular pathways (PERK, IREI, and ATF6) (Figure S5G). Since sleep fragmentation-induced ER stress involves ATF6 signaling,[70] and we had observed ATF6 overexpression in sleep-restricted women (Figures 2A and 2E–2G), we wondered if ATF6 expression could be altered in our hNSC models treated with the two metabolites. However, we did not find increased expression of ATF6 (Figure S5H); instead, we found higher mRNA levels of ATF4 and EIF2α, ER stress response genes downstream of the PERK pathway (Figure S5G), in metabolite-treated than in untreated hNSCs (Figure S5H). Notably, phosphorylated EIF2α protein, but not the total EIF2α protein, increases following metabolite treatments compared to untreated NSCs (Figure S5I). These data indicate that prolonged treatment of hNSCs with glutamic acid and methionine accumulated in sleep-restricted women resulted in stemness decline due to significant transcriptional alterations of NSC markers and genes associated with NSC proliferation and cell fate commitment, which converge at HSPA8 and the ER stress response pathway.

Metabolite-treated hNSCs demonstrate a reduced differentiation potential

The altered cell cycle profile (Figure 4) and the stemness decline (Figure 5) of metabolite-treated hNSCs suggest that hNSCs subjected to long-term glutamic acid and methionine treatment may have lost their differentiation potential. Therefore, we subjected FUCCI-hNSCs treated with metabolites for 30 days to further differentiation into neuronal and glial (oligodendrocytes and astrocytes) cell types using commercially available media systems, with metabolite supplementation every second day over an additional 10-day period (Figure 6A). Untreated hNSCs exhibited morphological changes within the initial 10 days of differentiation medium switch, particularly in neuronal and oligodendrocyte cells, accompanied by slower growth than untreated hNSCs maintained in neural expansion medium (NEM) (Figures 6B and S6A). Consistently, FACS analysis revealed an increased cell fraction in the G1 phase (red bars) and a smaller fraction of cells in S/G2/M (green bars) phases in untreated hNSC subjected to differentiation into three cell types versus untreated hNSCs maintained in NEM (Figures 6C and S6B). Furthermore, these differentiation cues induced elevated expression of DCX, OLIG2, and GFAP mRNA and proteins, serving as markers for neuronal, oligodendrocyte, and astrocyte cells, respectively, in untreated hNSCs (Figures 6D and 6E). In contrast, hNSCs under glutamic acid and methionine treatments, when subjected to differentiation into neuronal and oligodendrocyte cell types for 10 days, exhibited minimal morphological differences compared to untreated hNSCs. However, astrocyte differentiation in the presence of glutamic acid showed a tremendous amount of cell death (Figures 6B and S6A). Remarkably, the differentiated cells under glutamic acid and methionine treatments displayed a substantially lower red population (G1) and a markedly increased yellow population (G1/S checkpoints) compared to untreated hNSCs (Figures 6C and S6B). Regarding DCX, OLIG2, and GFAP gene expression, while methionine treatment led to a slight increase in respective cell type markers, consistent with morphological changes, glutamic acid treatment demonstrated the most striking differences, with marker levels significantly lower than those in untreated hNSCs (Figures 6D and 6E). These findings indicate that the long-term treatments with glutamic acid and methionine at concentrations observed in women after mild, prolonged sleep restriction impair hNSC differentiation potential.

DISCUSSION

More than a third of the adult population curtails their sleep routinely, thinking that such behavior does not have biological

(E) qRT-PCR and western blot analysis of PAX6 expression in the indicated samples. For qRT-PCR, the expression was relative to untreated hNSCs, and GAPDH was used as a housekeeping gene. For the western blot, VINCULIN was used as housekeeping control. See STAR Methods for primer sequences. *P*-values were calculated using a t-test.

(F) Venn diagram shows an intersection of upregulated genes from glutamic acid and methionine-treated FUCCI-hNSCs from (A) with upregulated restricted sleep proteomics candidates from (2A). Overlapping genes/proteins are indicated.

(G) Bar plot showing mRNA levels of HSPA8 using RNA-seq data.

(H) A bar plot represents a western blot showing HSPA8 protein levels in indicated samples and band quantifications. See also Figure S5.

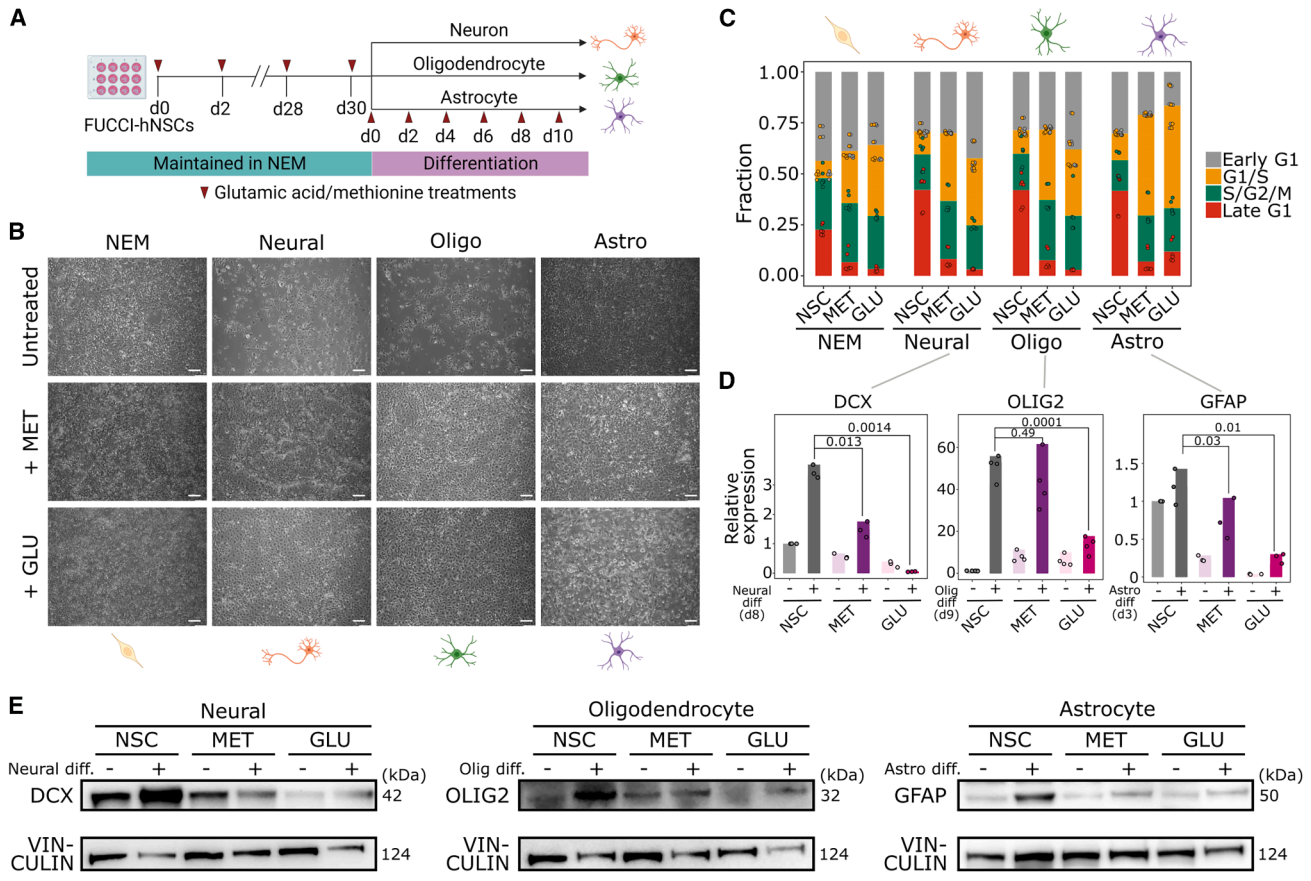

Figure 6. Long-term glutamic acid- and methionine-treated hNSCs show differentiation defects

(A) Schematic representation of differentiation of glutamic acid or methionine treated and untreated FUCCI-hNSC into neurons, astrocytes, and oligodendrocytes. Triangles represent time points (days) of fresh glutamic acid or methionine addition to the medium. NEM: neural expansion medium.

(B) Representative phase-contrast images of the untreated and glutamic acid or methionine-treated FUCCI-hNSC at day 10 of differentiation into indicated cell types. The scale bar is 100 μm.

(C) Flow cytometry analysis-based quantification of the relative proportion of cell-cycle phases from control and treated FUCCI-hNSCs undergoing differentiation into indicated cell types. Data points represent (n = 3 biological and 2 technical replicates) per sample.

(D and E) qRT-PCR analysis (D) and western blots (E) of neural (DCX), oligodendrocytes (OLIG2), and astrocytes (GFAP) markers at the indicated days of FUCCI-hNSC differentiation. The expression is relative to hNSCs maintained in neural expansion medium, and GAPDH was used as a housekeeping gene. See STAR Methods for primer sequences. p-values were calculated using a t-test. See also Figure S6.

consequences because they still appear "healthy". Sleep patterns and their health implications exhibit notable sex differences. Women generally require more sleep[42,43] and face higher risks of sleep disorders, mood disturbances, and adverse health outcomes from sleep deprivation compared to men.[44,47,48,52] These disparities underscore the importance of sex-specific considerations in sleep research and clinical approaches. Our clinical trial was previously designed to address this health disparity in women. Capitalizing on the randomized crossover design and employing a multiomics approach, we established a causal relationship between mild, "real-life" sleep restriction and stress-like proteomic and metabolic profiles in plasma.

It is worth pointing out that no changes in diet habits or body weight were observed across study phases during the trial and that no significant differences in metabolic equivalents (METs), Body Mass Index (BMI), blood pressure, cortisol levels, step counts, or moderate to vigorous physical activity (MVPA) before and after sleep restriction in the same participants.[53,54] Thus, our metabolomics findings directly reflect the effects of AS versus RS in this population. Compared to AS, sleep restriction increased proteins associated with protein folding, heat shock, and ER stress (Figure 7A, left panel). ER stress is associated with upregulated amino acid biosynthesis to cope with protein expression demands.[80,88] In particular, glutamic acid and methionine were enriched after sleep restriction (Figure 7A, right panel), consistent with previous reports.[35,82,83] Long-term treatment of these two amino acids resulted in nearly identical molecular signatures involving a high proliferation rate of hNSCs and a shortened G1 cell cycle concomitant with a pronounced decline in hNSC stemness that toppled both their maintenance and differentiation into neurons, oligodendrocytes, and astrocytes. This suggests a possible role of enrichment of these amino acids in cognitive decline associated with insufficient sleep.[89–91] Whether and how an excessive production of amino acids during

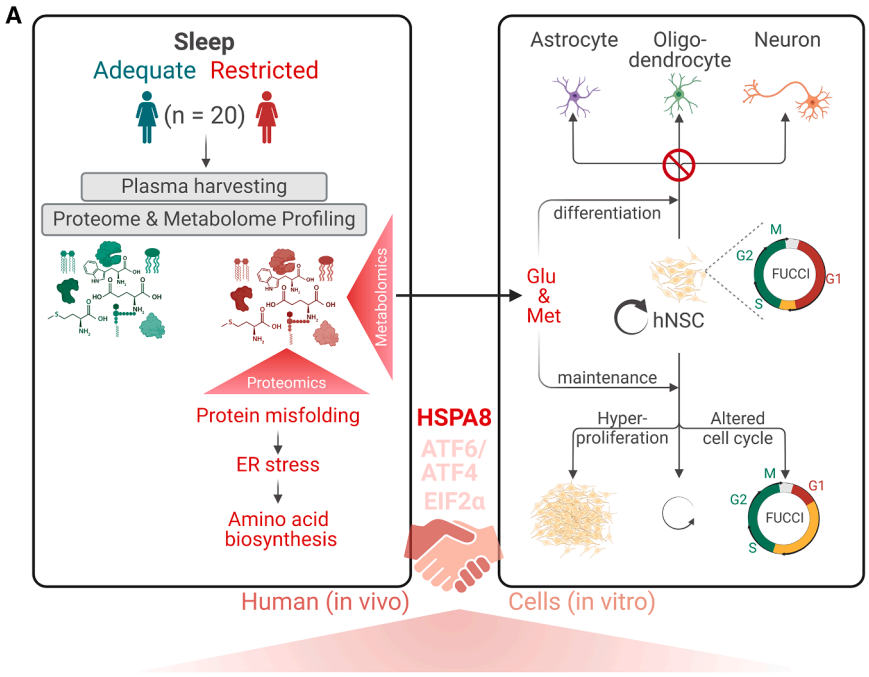

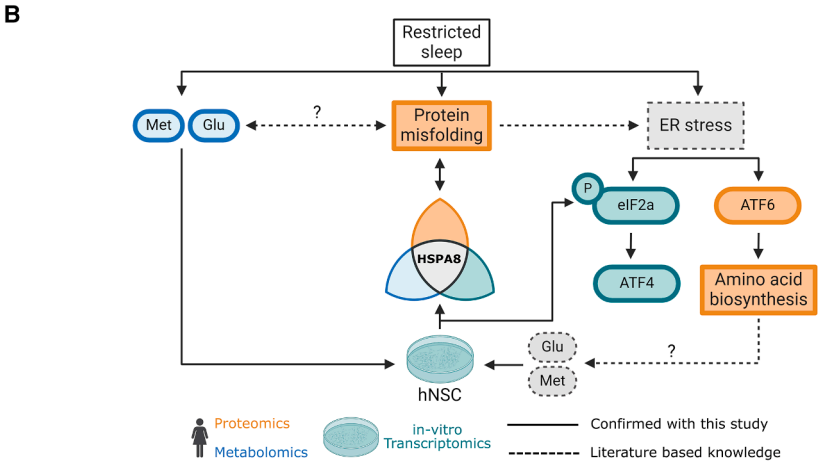

Figure 7. Summary models for this study

(A) Schematic representation of proteomics and metabolomic experiments on plasma from AS and RS women (left) and findings from glutamic acid and methionine treatments on FUCCI-hNSCs during their maintenance and differentiation (right).

(B) A summary model depicting findings from metabolomic and proteomic studies of AS and RS women plasma (*in vivo*) and glutamic acid and methionine treated hNSCs (*in vitro*) leading to activation of ER stress and identification of HSPA8 protein as a key candidate bridging the *in vivo* and *in vitro* studies.

insufficient sleep leads to aberration in protein synthesis and stability or even triggers protein misfolding remains to be addressed.

Role of HSPA8 in restricted sleep-induced stress response

HSPA8 provides the primary "handshake" between our proteomics from sleep-restricted women and the RNA-seq analysis of long-term metabolite-treated hNSCs (Figure 7A). As a chaperone protein, HSPA8 plays a vital role in maintaining protein homeostasis, particularly under stress conditions, and is upregulated in RS conditions in birds,[66] rodents,[31,33,67,92] and humans.[68] Our findings suggest that the upregulation of HSPA8 may represent a compensatory mechanism to counteract the protein misfolding and aggregation induced by sleep restriction. Our findings and the prior prediction of HSPA8 as a key blood mRNA biomarker of chronic insufficient sleep in humans[68] make HSPA8 a promising biomarker for sleep restriction. We deem it a potential therapeutic target for mitigating the adverse effects of sleep deprivation on cellular health, which warrants future investigations.

Conserved ATF4/6 and ER stress response in insufficient sleep

Our comprehensive multiomics approach validates the conservation of ER stress response activation following sleep restriction in women with findings reported in previous studies involving different species, including fruit flies,[93,94] birds,[95] and rodents.[96–98] Misfolded proteins, known triggers for ER stress, activate ATF6, a central player in ER stress response[69] associated with amino acid biosynthesis[80] (Figures 2G and 7B). Interestingly, our *in vitro* glutamic acid and methionine treatments also led to increased expression of phosphorylated-eIF2α and ATF4, representing additional facets of the ER stress (Figure 7B). Our findings align well with numerous studies exploring the impact of sleep restriction on the human proteome.[32,33,38,64,65] This convergence strengthens our *in vivo* and *in vitro* findings and emphasizes the universality of the stress response triggered by sleep restriction. Importantly, our multiomics approach identifying HSPA8/ATF6 from proteomics and HSPA8/ATF4 from metabolite-treated hNSC transcriptomes provides mechanistic insight into network alterations in sleep restriction. Well-known ATF6 targets and interacting proteins, including antioxidants (PRDX1/6), heat shock protein (HSPA5/8), chaperone protein (PDIA3), and HIF-1 signaling-related proteins (ALDOA, ENO1, and GAPDH) were upregulated after RS in women (Figures 2F and 2G). As ATF6 signaling is part of sleep fragmentation-induced ER stress[70] and is proposed to convey adaptation to long-term chronic stress rather than being decisive for cell fate determination,[99,100] future studies are warranted to dissect how ATF6 and its interacting proteins regulate target genes in sleep restriction mechanistically.

Additional pathways related to restricted sleep

After sleep restriction, NF-κB pathway-associated proteins like PPIA, NTRK2, MTPN, PARK7, and S100A8 were upregulated. Our recent report of activated NF-κB in endothelial cells after sleep restriction in women[53,54] and other reports in rat forebrain[101] and human peripheral blood mononuclear cells[64,102] corroborated this. The enrichment of proteins associated with NF-κB activation and pathways like "cellular remodeling" and "protein stability and ubiquitin pathway" in sleep-restricted conditions indicates a potential for cellular remodeling through stress-mediated pathways.

From metabolomics, we noticed an enrichment of trigonelline and fatty acids while reducing tri and di-glycerides in RS conditions (Figures 1C and 1D). Trigonelline, an arousal- and alertness-inducing bioactive molecule from coffee beans,[103] was reported to be upregulated in the human urine metabolome after sleep deprivation.[104] Similarly, non-esterified fatty acids were increased,[105,106] while triglycerides were decreased,[107] after sleep restriction in young adult men, concordant with our observations in women. Whether and how induction or repression of these proteins and metabolites may be associated with AS versus RS warrants future studies.

Prolonged sleep restriction has been linked to aging-related diseases (e.g., dementia) and a 12% higher risk of mortality.[90,108] We identified three proteins, CALML5, GAPDH, and LRP1, associated with the GO term "Alzheimer's disease" based on altered proteins and metabolite levels upon sleep restriction (Figure 3A). Further analysis revealed that LRP1 mRNA levels decreased significantly with glutamic acid and methionine treatment, GAPDH was mildly activated, and CALML5 was not expressed in NSCs (Figure S6C). LRP1 is known to play a protective role against neurodegeneration, with its reduced levels linked to blood-brain barrier breakdown, cognitive decline, Alzheimer's disease, and aging.[109–112] While these findings suggest a potential link between mild sleep restriction and aging-related phenotypes, we are mindful that such a functional link may not be direct due to the following caveats. Based on NIH Toolbox Cognition Domain assessments, no significant cognitive decline was observed in the healthy, young participants (ages 21–35) of our sleep restriction trial. Additionally, aging-related outcomes typically manifest after years or decades of sleep curtailment, which cannot be extrapolated from the 6-week study.

Similarly, we observed an enrichment of the GO term "Circadian entrainment" in our joint network pathway analysis based on altered protein and metabolite levels upon sleep restriction (Figure 3A). We identified CALML5 as an altered protein and glutamic acid and a diacylglycerol [DG(16:0/18:1(11Z)/0:0)] as metabolites within the "Circadian entrainment" GO upon sleep restriction. Glutamic acid and diacylglycerols have been reported to be under circadian rhythmic control for amino acid and lipid metabolism. Glutamate (the ionic form of glutamic acid, one of our leading tested candidates) conveys light information from the retina to the SCN,[113] and significant 24-h oscillations of extracellular glutamate have been observed in various brain regions, including the hippocampus and suprachiasmatic nucleus (SCN).[114] However, neither CALML5 nor DG(16:0/18:1(11Z)/0:0) has been previously reported in sleep restriction, and we did not detect any expression changes of CALML5 in glutamic acid-treated NSC models. Although significant literature links circadian rhythm disturbances, especially those caused by severe sleep deprivation, with NSC functions and various neurological diseases,[115–117] *in vitro* NSC models amenable to circadian rhythm manipulations are currently unavailable to test these candidates from our mild sleep restriction studies.

Limitations of the study

While our findings are robust, they are limited by the focus on a specific demographic (young women) and the *in vitro* 2D nature of hNSC experiments. Future studies should explore these phenomena in more diverse populations and through 3D organoids and *in vivo* models. Additionally, investigating the long-term neurological consequences of chronic sleep restriction would be of significant interest. However, long (perhaps years) experimental sleep restriction intervention is unethical and, therefore, not feasible. Future studies should also expand beyond amino acids to explore other metabolites and proteins affected by sleep restriction. Our current focus is primarily on the upregulated metabolites from RS and their negative impact on hNSCs. However, in women with AS, there is a possibility that beneficial metabolites and proteins are upregulated while harmful ones are downregulated. Conversely, in women experiencing RS, there is likely a downregulation of beneficial metabolites and proteins. Investigating additional proteomics and metabolomics candidates' combinatorial effects by applying genetic manipulations (on proteomics candidates) and prolonged treatment (on metabolomics candidates) will deepen our understanding of sleep restriction's impact on health.

In conclusion, our study demonstrates that mild, prolonged sleep restriction, practiced by a third of the adult population, induces a stress-like metabolomic and proteomic profile in healthy young women. Treatment of NSCs with candidate metabolites enriched in sleep restriction altered NSC stemness, suggesting that insufficient sleep may impair adult NSC differentiation and emphasizing the need for adequate sleep to maintain health and prevent neurological impairments.

RESOURCE AVAILABILITY

Lead contact

Further information and any requests should be directed to and will be fulfilled by the lead contact, Prof. Jianlong Wang (jw3925@cumc.columbia.edu).

Materials availability

This study did not generate new unique materials.

Data and code availability

Data: Sequencing data (RNA-seq) supporting this study's findings are available in Gene Expression Omnibus. The study's accession number is GSE254828. The metabolomic and proteomic datasets are provided in Tables S2 and S4, respectively.
Code: this paper does not report the original code.
Additional Information: any additional information required to reanalyze the data reported in this paper is available from the lead contact upon request.

ACKNOWLEDGMENTS

We thank Dr. Stephen Dalton for the FUCCI-hESC cell line, Drs. Benjamin Izar and Johannes Melms for their help with the CD7 live cell imaging platform, and

Dr. Riddhi Shah for providing details related to plasma samples. This publication was supported by the Biomarkers Core Laboratory at the Irving Institute for Clinical and Translational Research, home to Columbia University's Clinical and Translational Science Award. The research reported in this publication was carried out on the CCTI flow cytometry core, partially supported by the Office of the Director of the National Institutes of Health under the award S10RR027050. The content is solely the authors' responsibility and does not necessarily represent the official views of the National Institutes of Health. These studies used the resources of the Cancer Center Flow Core Facility, funded partly through the Center Grant P30CA013696. This work was supported by the seed fund of the Department of Medicine at Columbia University Irving Medical Center (J.W.) and by NIH/NHLBI R01HL106041, R01HL137234, and AHA 16SFRN29050000 (S.J.). Research in the Wang laboratory was also supported by NIH R01HD114122, R01HD095938, R01HD097268, and R21HD116446 (J.W.).

AUTHOR CONTRIBUTIONS

V.M. designed and performed experiments as well as multiomics data analysis; R.K.S. performed proteomics and R.B. western blot experiments; V.M. and X.H. analyzed RNA-seq data; H.Z., D.W.L., and S.J. provided reagents and resources; V.M. wrote the manuscript; S.J. provided critical input for the manuscript; J.W. conceived the project, designed the experiments, and approved the manuscript with input from all other authors.

DECLARATION OF INTERESTS

The authors declare no competing interests.

DECLARATION OF GENERATIVE AI AND AI-ASSISTED TECHNOLOGIES

While preparing this work, the author(s) used ChatGPT and Perplexity to refine the language. After using this tool, the author(s) reviewed and edited the content as needed and take full responsibility for the content of the publication.

STAR★METHODS

Detailed methods are provided in the online version of this paper and include the following:

- KEY RESOURCES TABLE
- EXPERIMENTAL MODEL AND STUDY PARTICIPANT DETAILS
  - Study participants, sleep restriction intervention, and plasma samples
  - Cell culture of FUCCI-hESCs
  - Differentiation of FUCCI-hESCs to FUCCI-NSCs
  - Differentiation of FUCCI-NSCs to neural, oligodendrocytes, and astrocytes
- METHOD DETAILS
  - Targeted metabolomics and data analysis
  - Proteomics and data analysis
  - Metabolites treatment
  - Live cell imaging and cell proliferation analysis pipeline
  - Quantitative real-time reverse transcription PCR
  - Flow cytometry
  - RNA-sequencing and data analysis
  - Western blotting
  - Cell proliferation assay (MTT-based)
  - Schematic representations
- QUANTIFICATION AND STATISTICAL ANALYSIS
- ADDITIONAL RESOURCES

SUPPLEMENTAL INFORMATION

Supplemental information can be found online at https://doi.org/10.1016/j.isci.2025.112510.

Received: March 1, 2024
Revised: January 8, 2025
Accepted: April 18, 2025
Published: April 22, 2025

REFERENCES

1. Hirshkowitz, M., Whiton, K., Albert, S.M., Alessi, C., Bruni, O., DonCarlos, L., Hazen, N., Herman, J., Katz, E.S., Kheirandish-Gozal, L., et al. (2015). National Sleep Foundation's sleep time duration recommendations: methodology and results summary. Sleep Health *1*, 40–43. https://doi.org/10.1016/j.sleh.2014.12.010.
2. Watson, N.F., Badr, M.S., Belenky, G., Bliwise, D.L., Buxton, O.M., Buysse, D., Dinges, D.F., Gangwisch, J., Grandner, M.A., Kushida, C., et al. (2015). Recommended Amount of Sleep for a Healthy Adult: A Joint Consensus Statement of the American Academy of Sleep Medicine and Sleep Research Society. Sleep *38*, 843–844. https://doi.org/10.5665/sleep.4716.
3. Lane, J.M., Qian, J., Mignot, E., Redline, S., Scheer, F.A.J.L., and Saxena, R. (2023). Genetics of circadian rhythms and sleep in human health and disease. Nat. Rev. Genet. *24*, 4–20. https://doi.org/10.1038/s41576-022-00519-z.
4. Cracco, L., Appleby, B.S., and Gambetti, P. (2018). Fatal familial insomnia and sporadic fatal insomnia. Handb. Clin. Neurol. *153*, 271–299. https://doi.org/10.1016/B978-0-444-63945-5.00015-5.
5. Sang, D., Lin, K., Yang, Y., Ran, G., Li, B., Chen, C., Li, Q., Ma, Y., Lu, L., Cui, X.Y., et al. (2023). Prolonged sleep deprivation induces a cytokine-storm-like syndrome in mammals. Cell *186*, 5500–5516.e21. https://doi.org/10.1016/j.cell.2023.10.025.
6. Vaccaro, A., Kaplan Dor, Y., Nambara, K., Pollina, E.A., Lin, C., Greenberg, M.E., and Rogulja, D. (2020). Sleep Loss Can Cause Death through Accumulation of Reactive Oxygen Species in the Gut. Cell *181*, 1307–1328.e15. https://doi.org/10.1016/j.cell.2020.04.049.
7. Liu, G.H., and Qu, J. (2022). Longevity secret: A pluripotent superpower. Cell Metab. *34*, 803–804. https://doi.org/10.1016/j.cmet.2022.05.001.
8. Lu, J.Y., Simon, M., Zhao, Y., Ablaeva, J., Corson, N., Choi, Y., Yamada, K.Y.H., Schork, N.J., Hood, W.R., Hill, G.E., et al. (2022). Comparative transcriptomics reveals circadian and pluripotency networks as two pillars of longevity regulation. Cell Metab. *34*, 836–856.e5. https://doi.org/10.1016/j.cmet.2022.04.011.
9. Tulina, N.M., Chen, W.F., Chen, J.H., Sowcik, M., and Sehgal, A. (2014). Day-night cycles and the sleep-promoting factor, Sleepless, affect stem cell activity in the Drosophila testis. Proc. Natl. Acad. Sci. USA *111*, 3026–3031. https://doi.org/10.1073/pnas.1316552111.
10. Boucher, H., Vanneaux, V., Domet, T., Parouchev, A., and Larghero, J. (2016). Circadian Clock Genes Modulate Human Bone Marrow Mesenchymal Stem Cell Differentiation, Migration and Cell Cycle. PLoS One *11*, e0146674. https://doi.org/10.1371/journal.pone.0146674.
11. Lu, C., Yang, Y., Zhao, R., Hua, B., Xu, C., Yan, Z., Sun, N., and Qian, R. (2016). Role of circadian gene Clock during differentiation of mouse pluripotent stem cells. Protein Cell *7*, 820–832. https://doi.org/10.1007/s13238-016-0319-9.
12. Zagni, C., Almeida, L.O., Balan, T., Martins, M.T., Rosselli-Murai, L.K., Papagerakis, P., Castilho, R.M., and Squarize, C.H. (2017). PTEN Mediates Activation of Core Clock Protein BMAL1 and Accumulation of Epidermal Stem Cells. Stem Cell Rep. *9*, 304–314. https://doi.org/10.1016/j.stemcr.2017.05.006.
13. Janich, P., Pascual, G., Merlos-Suárez, A., Batlle, E., Ripperger, J., Albrecht, U., Cheng, H.Y.M., Obrietan, K., Di Croce, L., and Benitah, S.A. (2011). The circadian molecular clock creates epidermal stem cell heterogeneity. Nature *480*, 209–214. https://doi.org/10.1038/nature10649.
14. Kimiwada, T., Sakurai, M., Ohashi, H., Aoki, S., Tominaga, T., and Wada, K. (2009). Clock genes regulate neurogenic transcription factors, including NeuroD1, and the neuronal differentiation of adult neural

stem/progenitor cells. Neurochem. Int. *54*, 277–285. https://doi.org/10.1016/j.neuint.2008.12.005.

15. Borgs, L., Beukelaers, P., Vandenbosch, R., Nguyen, L., Moonen, G., Maquet, P., Albrecht, U., Belachew, S., and Malgrange, B. (2009). Period 2 regulates neural stem/progenitor cell proliferation in the adult hippocampus. BMC Neurosci. *10*, 30. https://doi.org/10.1186/1471-2202-10-30.
16. McAlpine, C.S., Kiss, M.G., Rattik, S., He, S., Vassalli, A., Valet, C., Anzai, A., Chan, C.T., Mindur, J.E., Kahles, F., et al. (2019). Sleep modulates haematopoiesis and protects against atherosclerosis. Nature *566*, 383–387. https://doi.org/10.1038/s41586-019-0948-2.
17. McAlpine, C.S., Kiss, M.G., Zuraikat, F.M., Cheek, D., Schiroli, G., Amatullah, H., Huynh, P., Bhatti, M.Z., Wong, L.P., Yates, A.G., et al. (2022). Sleep exerts lasting effects on hematopoietic stem cell function and diversity. J. Exp. Med. *219*, e20220081. https://doi.org/10.1084/jem.20220081.
18. Tall, A.R., and Jelic, S. (2019). How broken sleep promotes cardiovascular disease. Nature *566*, 329–330. https://doi.org/10.1038/d41586-019-00393-6.
19. Rolls, A., Pang, W.W., Ibarra, I., Colas, D., Bonnavion, P., Korin, B., Heller, H.C., Weissman, I.L., and de Lecea, L. (2015). Sleep disruption impairs haematopoietic stem cell transplantation in mice. Nat. Commun. *6*, 8516. https://doi.org/10.1038/ncomms9516.
20. Li, S., Tang, L., Zhou, J., Anchouche, S., Li, D., Yang, Y., Liu, Z., Wu, J., Hu, J., Zhou, Y., et al. (2022). Sleep deprivation induces corneal epithelial progenitor cell over-expansion through disruption of redox homeostasis in the tear film. Stem Cell Rep. *17*, 1105–1119. https://doi.org/10.1016/j.stemcr.2022.03.017.
21. Jelic, S., Lederer, D.J., Adams, T., Padeletti, M., Colombo, P.C., Factor, P., and Le Jemtel, T.H. (2009). Endothelial repair capacity and apoptosis are inversely related in obstructive sleep apnea. Vasc. Health Risk Manag. *5*, 909–920. https://doi.org/10.2147/vhrm.s8123.
22. Jelic, S., Padeletti, M., Kawut, S.M., Higgins, C., Canfield, S.M., Onat, D., Colombo, P.C., Basner, R.C., Factor, P., and LeJemtel, T.H. (2008). Inflammation, oxidative stress, and repair capacity of the vascular endothelium in obstructive sleep apnea. Circulation *117*, 2270–2278. https://doi.org/10.1161/CIRCULATIONAHA.107.741512.
23. Elkhenany, H., AlOkda, A., El-Badawy, A., and El-Badri, N. (2018). Tissue regeneration: Impact of sleep on stem cell regenerative capacity. Life Sci. *214*, 51–61. https://doi.org/10.1016/j.lfs.2018.10.057.
24. Gupta, P., Hourigan, K., Jadhav, S., Bellare, J., and Verma, P. (2017). Effect of lactate and pH on mouse pluripotent stem cells: Importance of media analysis. Biochem. Eng. J. *118*, 25–33. https://doi.org/10.1016/j.bej.2016.11.005.
25. Lu, V., Roy, I.J., Torres, A., Jr., Joly, J.H., Ahsan, F.M., Graham, N.A., and Teitell, M.A. (2022). Glutamine-dependent signaling controls pluripotent stem cell fate. Dev. Cell *57*, 610–623.e8. https://doi.org/10.1016/j.devcel.2022.02.003.
26. Marsboom, G., Zhang, G.F., Pohl-Avila, N., Zhang, Y., Yuan, Y., Kang, H., Hao, B., Brunengraber, H., Malik, A.B., and Rehman, J. (2016). Glutamine Metabolism Regulates the Pluripotency Transcription Factor OCT4. Cell Rep. *16*, 323–332. https://doi.org/10.1016/j.celrep.2016.05.089.
27. Aho, V., Ollila, H.M., Kronholm, E., Bondia-Pons, I., Soininen, P., Kangas, A.J., Hilvo, M., Seppälä, I., Kettunen, J., Oikonen, M., et al. (2016). Prolonged sleep restriction induces changes in pathways involved in cholesterol metabolism and inflammatory responses. Sci. Rep. *6*, 24828. https://doi.org/10.1038/srep24828.
28. Chua, E.C.P., Shui, G., Cazenave-Gassiot, A., Wenk, M.R., and Gooley, J.J. (2015). Changes in Plasma Lipids during Exposure to Total Sleep Deprivation. Sleep *38*, 1683–1691. https://doi.org/10.5665/sleep.5142.
29. Davies, S.K., Ang, J.E., Revell, V.L., Holmes, B., Mann, A., Robertson, F.P., Cui, N., Middleton, B., Ackermann, K., Kayser, M., et al. (2014). Effect of sleep deprivation on the human metabolome. Proc. Natl. Acad. Sci. USA *111*, 10761–10766. https://doi.org/10.1073/pnas.1402663111.
30. Weljie, A.M., Meerlo, P., Goel, N., Sengupta, A., Kayser, M.S., Abel, T., Birnbaum, M.J., Dinges, D.F., and Sehgal, A. (2015). Oxalic acid and diacylglycerol 36:3 are cross-species markers of sleep debt. Proc. Natl. Acad. Sci. USA *112*, 2569–2574. https://doi.org/10.1073/pnas.1417432112.
31. Pawlyk, A.C., Ferber, M., Shah, A., Pack, A.I., and Naidoo, N. (2007). Proteomic analysis of the effects and interactions of sleep deprivation and aging in mouse cerebral cortex. J. Neurochem. *103*, 2301–2313. https://doi.org/10.1111/j.1471-4159.2007.04949.x.
32. Ren, J., Zhang, M.J., Li, T.M., Zhang, J.E., Lin, R., Chen, S., Luo, M., and Dong, M.Q. (2016). Quantitative Proteomics of Sleep-Deprived Mouse Brains Reveals Global Changes in Mitochondrial Proteins. PLoS One *11*, e0163500. https://doi.org/10.1371/journal.pone.0163500.
33. Simor, A., Györffy, B.A., Gulyássy, P., Völgyi, K., Tóth, V., Todorov, M.I., Kis, V., Borhegyi, Z., Szabó, Z., Janáky, T., et al. (2017). The short- and long-term proteomic effects of sleep deprivation on the cortical and thalamic synapses. Mol. Cell. Neurosci. *79*, 64–80. https://doi.org/10.1016/j.mcn.2017.01.002.
34. Yoon, S.J., Long, N.P., Jung, K.H., Kim, H.M., Hong, Y.J., Fang, Z., Kim, S.J., Kim, T.J., Anh, N.H., Hong, S.S., and Kwon, S.W. (2019). Systemic and Local Metabolic Alterations in Sleep-Deprivation-Induced Stress: A Multiplatform Mass-Spectrometry-Based Lipidomics and Metabolomics Approach. J. Proteome Res. *18*, 3295–3304. https://doi.org/10.1021/acs.jproteome.9b00234.
35. Bell, L.N., Kilkus, J.M., Booth, J.N., 3rd, Bromley, L.E., Imperial, J.G., and Penev, P.D. (2013). Effects of sleep restriction on the human plasma metabolome. Physiol. Behav. *122*, 25–31. https://doi.org/10.1016/j.physbeh.2013.08.007.
36. Depner, C.M., Cogswell, D.T., Bisesi, P.J., Markwald, R.R., Cruickshank-Quinn, C., Quinn, K., Melanson, E.L., Reisdorph, N., and Wright, K.P. (2020). Developing preliminary blood metabolomics-based biomarkers of insufficient sleep in humans. Sleep *43*, zsz321. https://doi.org/10.1093/sleep/zsz321.
37. van den Berg, R., Mook-Kanamori, D.O., Donga, E., van Dijk, M., van Dijk, J.G., Lammers, G.J., van Kralingen, K.W., Prehn, C., Adamski, J., Romijn, J.A., et al. (2016). A single night of sleep curtailment increases plasma acylcarnitines: Novel insights in the relationship between sleep and insulin resistance. Arch. Biochem. Biophys. *589*, 145–151. https://doi.org/10.1016/j.abb.2015.09.017.
38. Bjørkum, A.A., Carrasco Duran, A., Frode, B., Sinha Roy, D., Rosendahl, K., Birkeland, E., and Stuhr, L. (2021). Human blood serum proteome changes after 6 hours of sleep deprivation at night. Sleep Sci. Pract. *5*, zpae042. https://doi.org/10.1186/s41606-021-00066-2.
39. Hu, S., Li, P., Zhang, R., Liu, X., and Wei, S. (2021). Integrated metabolomics and proteomics analysis reveals energy metabolism disorders in the livers of sleep-deprived mice. J. Proteomics *245*, 104290. https://doi.org/10.1016/j.jprot.2021.104290.
40. Sengupta, A., Rhoades, S.D., Kim, E.J., Nayak, S., Grant, G.R., Meerlo, P., and Weljie, A.M. (2017). Sleep restriction induced energy, methylation and lipogenesis metabolic switches in rat liver. Int. J. Biochem. Cell Biol. *93*, 129–135. https://doi.org/10.1016/j.biocel.2017.08.014.
41. Humer, E., Pieh, C., and Brandmayr, G. (2020). Metabolomics in Sleep, Insomnia and Sleep Apnea. Int. J. Mol. Sci. *21*, 7244. https://doi.org/10.3390/ijms21197244.
42. Krishnan, V., and Collop, N.A. (2006). Gender differences in sleep disorders. Curr. Opin. Pulm. Med. *12*, 383–389. https://doi.org/10.1097/01.mcp.0000245705.69440.6a.
43. Mong, J.A., and Cusmano, D.M. (2016). Sex differences in sleep: impact of biological sex and sex steroids. Philos. Trans. R. Soc. Lond. B Biol. Sci. *371*, 20150110. https://doi.org/10.1098/rstb.2015.0110.
44. McLean, C.P., Asnaani, A., Litz, B.T., and Hofmann, S.G. (2011). Gender differences in anxiety disorders: prevalence, course of illness,

comorbidity and burden of illness. J. Psychiatr. Res. *45*, 1027–1035. https://doi.org/10.1016/j.jpsychires.2011.03.006.

45. Albert, P.R. (2015). Why is depression more prevalent in women? J. Psychiatry Neurosci. *40*, 219–221. https://doi.org/10.1503/jpn.150205.
46. Zhang, B., and Wing, Y.K. (2006). Sex differences in insomnia: a meta-analysis. Sleep *29*, 85–93. https://doi.org/10.1093/sleep/29.1.85.
47. Swanson, L.M., Pickett, S.M., Flynn, H., and Armitage, R. (2011). Relationships among depression, anxiety, and insomnia symptoms in perinatal women seeking mental health treatment. J. Womens Health *20*, 553–558. https://doi.org/10.1089/jwh.2010.2371.
48. Mallampalli, M.P., and Carter, C.L. (2014). Exploring sex and gender differences in sleep health: a Society for Women's Health Research Report. J. Womens Health *23*, 553–562. https://doi.org/10.1089/jwh.2014.4816.
49. Ferrie, J.E., Shipley, M.J., Cappuccio, F.P., Brunner, E., Miller, M.A., Kumari, M., and Marmot, M.G. (2007). A prospective study of change in sleep duration: associations with mortality in the Whitehall II cohort. Sleep *30*, 1659–1666. https://doi.org/10.1093/sleep/30.12.1659.
50. Ayas, N.T., White, D.P., Manson, J.E., Stampfer, M.J., Speizer, F.E., Malhotra, A., and Hu, F.B. (2003). A prospective study of sleep duration and coronary heart disease in women. Arch. Intern. Med. *163*, 205–209. https://doi.org/10.1001/archinte.163.2.205.
51. Cappuccio, F.P., Stranges, S., Kandala, N.B., Miller, M.A., Taggart, F.M., Kumari, M., Ferrie, J.E., Shipley, M.J., Brunner, E.J., and Marmot, M.G. (2007). Gender-specific associations of short sleep duration with prevalent and incident hypertension: the Whitehall II Study. Hypertension *50*, 693–700. https://doi.org/10.1161/HYPERTENSIONAHA.107.095471.
52. Irwin, M.R., Carrillo, C., and Olmstead, R. (2010). Sleep loss activates cellular markers of inflammation: sex differences. Brain Behav. Immun. *24*, 54–57. https://doi.org/10.1016/j.bbi.2009.06.001.
53. Shah, R., Shah, V.K., Emin, M., Gao, S., Sampogna, R.V., Aggarwal, B., Chang, A., St-Onge, M.P., Malik, V., Wang, J., et al. (2023). Mild sleep restriction increases endothelial oxidative stress in female persons. Sci. Rep. *13*, 15360. https://doi.org/10.1038/s41598-023-42758-y.
54. Shah, R., St-Onge, M.P., Emin, M., Gao, S., Sampogna, R.V., Aggarwal, B., Wei, Y., and Jelic, S. (2022). Sleep Deprivation Impairs Vascular Function in Healthy Women. Ann. Am. Thorac. Soc. *19*, 2097–2100. https://doi.org/10.1513/AnnalsATS.202205-406RL.
55. Tyanova, S., Temu, T., Sinitcyn, P., Carlson, A., Hein, M.Y., Geiger, T., Mann, M., and Cox, J. (2016). The Perseus computational platform for comprehensive analysis of (prote)omics data. Nat. Methods *13*, 731–740. https://doi.org/10.1038/nmeth.3901.
56. Zhou, Y., Zhou, B., Pache, L., Chang, M., Khodabakhshi, A.H., Tanaseichuk, O., Benner, C., and Chanda, S.K. (2019). Metascape provides a biologist-oriented resource for the analysis of systems-level datasets. Nat. Commun. *10*, 1523. https://doi.org/10.1038/s41467-019-09234-6.
57. Lambert, S.A., Jolma, A., Campitelli, L.F., Das, P.K., Yin, Y., Albu, M., Chen, X., Taipale, J., Hughes, T.R., and Weirauch, M.T. (2018). The Human Transcription Factors. Cell *172*, 650–665. https://doi.org/10.1016/j.cell.2018.01.029.
58. ENCODE Project Consortium (2012). An integrated encyclopedia of DNA elements in the human genome. Nature *489*, 57–74. https://doi.org/10.1038/nature11247.
59. Szklarczyk, D., Gable, A.L., Nastou, K.C., Lyon, D., Kirsch, R., Pyysalo, S., Doncheva, N.T., Legeay, M., Fang, T., Bork, P., et al. (2021). The STRING database in 2021: customizable protein-protein networks, and functional characterization of user-uploaded gene/measurement sets. Nucleic Acids Res. *49*, D605–D612. https://doi.org/10.1093/nar/gkaa1074.
60. Snel, B., Lehmann, G., Bork, P., and Huynen, M.A. (2000). STRING: a web-server to retrieve and display the repeatedly occurring neighbourhood of a gene. Nucleic Acids Res. *28*, 3442–3444. https://doi.org/10.1093/nar/28.18.3442.
61. Spiegel, K., Sheridan, J.F., and Van Cauter, E. (2002). Effect of Sleep Deprivation on Response to Immunizaton. JAMA *288*, 1471–1472. https://doi.org/10.1001/jama.288.12.1469.
62. Prather, A.A., Hall, M., Fury, J.M., Ross, D.C., Muldoon, M.F., Cohen, S., and Marsland, A.L. (2012). Sleep and antibody response to hepatitis B vaccination. Sleep *35*, 1063–1069. https://doi.org/10.5665/sleep.1990.
63. Lange, T., Dimitrov, S., Bollinger, T., Diekelmann, S., and Born, J. (2011). Sleep after vaccination boosts immunological memory. J. Immunol. *187*, 283–290. https://doi.org/10.4049/jimmunol.1100015.
64. Aho, V., Ollila, H.M., Rantanen, V., Kronholm, E., Surakka, I., van Leeuwen, W.M.A., Lehto, M., Matikainen, S., Ripatti, S., Härmä, M., et al. (2013). Partial sleep restriction activates immune response-related gene expression pathways: experimental and epidemiological studies in humans. PLoS One *8*, e77184. https://doi.org/10.1371/journal.pone.0077184.
65. Kim, J.H., Kim, J.H., Cho, Y.E., Baek, M.C., Jung, J.Y., Lee, M.G., Jang, I.S., Lee, H.W., and Suk, K. (2014). Chronic sleep deprivation-induced proteome changes in astrocytes of the rat hypothalamus. J. Proteome Res. *13*, 4047–4061. https://doi.org/10.1021/pr500431j.
66. Jones, S., Pfister-Genskow, M., Cirelli, C., and Benca, R.M. (2008). Changes in brain gene expression during migration in the white-crowned sparrow. Brain Res. Bull. *76*, 536–544. https://doi.org/10.1016/j.brainresbull.2008.03.008.
67. Vecsey, C.G., Peixoto, L., Choi, J.H.K., Wimmer, M., Jaganath, D., Hernandez, P.J., Blackwell, J., Meda, K., Park, A.J., Hannenhalli, S., and Abel, T. (2012). Genomic analysis of sleep deprivation reveals translational regulation in the hippocampus. Physiol. Genomics *44*, 981–991. https://doi.org/10.1152/physiolgenomics.00084.2012.
68. Laing, E.E., Moller-Levet, C.S., Dijk, D.J., and Archer, S.N. (2019). Identifying and validating blood mRNA biomarkers for acute and chronic insufficient sleep in humans: a machine learning approach. Sleep *42*, zsy186. https://doi.org/10.1093/sleep/zsy186.
69. Hillary, R.F., and FitzGerald, U. (2018). A lifetime of stress: ATF6 in development and homeostasis. J. Biomed. Sci. *25*, 48. https://doi.org/10.1186/s12929-018-0453-1.
70. Hakim, F., Wang, Y., Carreras, A., Hirotsu, C., Zhang, J., Peris, E., and Gozal, D. (2015). Chronic sleep fragmentation during the sleep period induces hypothalamic endoplasmic reticulum stress and PTP1b-mediated leptin resistance in male mice. Sleep *38*, 31–40. https://doi.org/10.5665/sleep.4320.
71. Howarth, D.L., Lindtner, C., Vacaru, A.M., Sachidanandam, R., Tsedensodnom, O., Vasilkova, T., Buettner, C., and Sadler, K.C. (2014). Activating transcription factor 6 is necessary and sufficient for alcoholic fatty liver disease in zebrafish. PLoS Genet. *10*, e1004335. https://doi.org/10.1371/journal.pgen.1004335.
72. Wang, S., Hu, B., Ding, Z., Dang, Y., Wu, J., Li, D., Liu, X., Xiao, B., Zhang, W., Ren, R., et al. (2018). ATF6 safeguards organelle homeostasis and cellular aging in human mesenchymal stem cells. Cell Discov. *4*, 2. https://doi.org/10.1038/s41421-017-0003-0.
73. Haze, K., Okada, T., Yoshida, H., Yanagi, H., Yura, T., Negishi, M., and Mori, K. (2001). Identification of the G13 (cAMP-response-element-binding protein-related protein) gene product related to activating transcription factor 6 as a transcriptional activator of the mammalian unfolded protein response. Biochem. J. *355*, 19–28. https://doi.org/10.1042/0264-6021:3550019.
74. Chong, J., Wishart, D.S., and Xia, J. (2019). Using MetaboAnalyst 4.0 for Comprehensive and Integrative Metabolomics Data Analysis. Curr. Protoc. Bioinformatics *68*, e86. https://doi.org/10.1002/cpbi.86.
75. Pang, Z., Chong, J., Zhou, G., de Lima Morais, D.A., Chang, L., Barrette, M., Gauthier, C., Jacques, P.É., Li, S., and Xia, J. (2021). MetaboAnalyst 5.0: narrowing the gap between raw spectra and functional insights. Nucleic Acids Res. *49*, W388–W396. https://doi.org/10.1093/nar/gkab382.

76. Xia, J., and Wishart, D.S. (2011). Web-based inference of biological patterns, functions and pathways from metabolomic data using MetaboAnalyst. Nat. Protoc. *6*, 743–760. https://doi.org/10.1038/nprot.2011.319.

77. Singh, A.M., Chappell, J., Trost, R., Lin, L., Wang, T., Tang, J., Matlock, B.K., Weller, K.P., Wu, H., Zhao, S., et al. (2013). Cell-cycle control of developmentally regulated transcription factors accounts for heterogeneity in human pluripotent cells. Stem Cell Rep. *1*, 532–544. https://doi.org/10.1016/j.stemcr.2013.10.009.

78. Sakaue-Sawano, A., Kurokawa, H., Morimura, T., Hanyu, A., Hama, H., Osawa, H., Kashiwagi, S., Fukami, K., Miyata, T., Miyoshi, H., et al. (2008). Visualizing spatiotemporal dynamics of multicellular cell-cycle progression. Cell *132*, 487–498. https://doi.org/10.1016/j.cell.2007.12.033.

79. Furutachi, S., Miya, H., Watanabe, T., Kawai, H., Yamasaki, N., Harada, Y., Imayoshi, I., Nelson, M., Nakayama, K.I., Hirabayashi, Y., and Gotoh, Y. (2015). Slowly dividing neural progenitors are an embryonic origin of adult neural stem cells. Nat. Neurosci. *18*, 657–665. https://doi.org/10.1038/nn.3989.

80. Gonen, N., Meller, A., Sabath, N., and Shalgi, R. (2019). Amino Acid Biosynthesis Regulation during Endoplasmic Reticulum Stress Is Coupled to Protein Expression Demands. iScience *19*, 204–213. https://doi.org/10.1016/j.isci.2019.07.022.

81. Zaragoza, R. (2020). Transport of Amino Acids Across the Blood-Brain Barrier. Front. Physiol. *11*, 973. https://doi.org/10.3389/fphys.2020.00973.

82. Watson, C.J., Lydic, R., and Baghdoyan, H.A. (2011). Sleep duration varies as a function of glutamate and GABA in rat pontine reticular formation. J. Neurochem. *118*, 571–580. https://doi.org/10.1111/j.1471-4159.2011.07350.x.

83. Dash, M.B., Douglas, C.L., Vyazovskiy, V.V., Cirelli, C., and Tononi, G. (2009). Long-term homeostasis of extracellular glutamate in the rat cerebral cortex across sleep and waking states. J. Neurosci. *29*, 620–629. https://doi.org/10.1523/JNEUROSCI.5486-08.2009.

84. Stirling, D.R., Swain-Bowden, M.J., Lucas, A.M., Carpenter, A.E., Cimini, B.A., and Goodman, A. (2021). CellProfiler 4: improvements in speed, utility and usability. BMC Bioinf. *22*, 433. https://doi.org/10.1186/s12859-021-04344-9.

85. Pauklin, S., and Vallier, L. (2013). The cell-cycle state of stem cells determines cell fate propensity. Cell *155*, 135–147. https://doi.org/10.1016/j.cell.2013.08.031.

86. Salomoni, P., and Calegari, F. (2010). Cell cycle control of mammalian neural stem cells: putting a speed limit on G1. Trends Cell Biol. *20*, 233–243. https://doi.org/10.1016/j.tcb.2010.01.006.

87. Wang, C., Zhang, X., Wang, X., Zhai, Y., Li, M., Pan, J., Bai, Y., Rong, X., and Zhou, J. (2022). Genetic deletion of hspa8 leads to selective tissue malformations in zebrafish embryonic development. J. Cell Sci. *135*, jcs259734. https://doi.org/10.1242/jcs.259734.

88. Harding, H.P., Zhang, Y., Zeng, H., Novoa, I., Lu, P.D., Calfon, M., Sadri, N., Yun, C., Popko, B., Paules, R., et al. (2003). An integrated stress response regulates amino acid metabolism and resistance to oxidative stress. Mol. Cell *11*, 619–633. https://doi.org/10.1016/s1097-2765(03)00105-9.

89. Li, Y., Sahakian, B.J., Kang, J., Langley, C., Zhang, W., Xie, C., Xiang, S., Yu, J., Cheng, W., and Feng, J. (2022). The brain structure and genetic mechanisms underlying the nonlinear association between sleep duration, cognition and mental health. Nat. Aging *2*, 425–437. https://doi.org/10.1038/s43587-022-00210-2.

90. Sabia, S., Fayosse, A., Dumurgier, J., van Hees, V.T., Paquet, C., Sommerlad, A., Kivimäki, M., Dugravot, A., and Singh-Manoux, A. (2021). Association of sleep duration in middle and old age with incidence of dementia. Nat. Commun. *12*, 2289. https://doi.org/10.1038/s41467-021-22354-2.

91. Yeo, S.C., Lai, C.K.Y., Tan, J., Lim, S., Chandramoghan, Y., Tan, T.K., and Gooley, J.J. (2023). Early morning university classes are associated with impaired sleep and academic performance. Nat. Hum. Behav. *7*, 502–514. https://doi.org/10.1038/s41562-023-01531-x.

92. Urquhart, K.R., Zhao, Y., Baker, J.A., Lu, Y., Yan, L., Cook, M.N., Jones, B.C., Hamre, K.M., and Lu, L. (2016). A novel heat shock protein alpha 8 (Hspa8) molecular network mediating responses to stress- and ethanol-related behaviors. Neurogenetics *17*, 91–105. https://doi.org/10.1007/s10048-015-0470-0.

93. Shaw, P.J., Cirelli, C., Greenspan, R.J., and Tononi, G. (2000). Correlates of sleep and waking in Drosophila melanogaster. Science *287*, 1834–1837. https://doi.org/10.1126/science.287.5459.1834.

94. Naidoo, N., Casiano, V., Cater, J., Zimmerman, J., and Pack, A.I. (2007). A role for the molecular chaperone protein BiP/GRP78 in Drosophila sleep homeostasis. Sleep *30*, 557–565. https://doi.org/10.1093/sleep/30.5.557.

95. Jones, S., Pfister-Genskow, M., Benca, R.M., and Cirelli, C. (2008). Molecular correlates of sleep and wakefulness in the brain of the white-crowned sparrow. J. Neurochem. *105*, 46–62. https://doi.org/10.1111/j.1471-4159.2007.05089.x.

96. Cirelli, C., Gutierrez, C.M., and Tononi, G. (2004). Extensive and divergent effects of sleep and wakefulness on brain gene expression. Neuron *41*, 35–43. https://doi.org/10.1016/s0896-6273(03)00814-6.

97. Mackiewicz, M., Shockley, K.R., Romer, M.A., Galante, R.J., Zimmerman, J.E., Naidoo, N., Baldwin, D.A., Jensen, S.T., Churchill, G.A., and Pack, A.I. (2007). Macromolecule biosynthesis: a key function of sleep. Physiol. Genomics *31*, 441–457. https://doi.org/10.1152/physiolgenomics.00275.2006.

98. Naidoo, N., Giang, W., Galante, R.J., and Pack, A.I. (2005). Sleep deprivation induces the unfolded protein response in mouse cerebral cortex. J. Neurochem. *92*, 1150–1157. https://doi.org/10.1111/j.1471-4159.2004.02952.x.

99. Shoulders, M.D., Ryno, L.M., Genereux, J.C., Moresco, J.J., Tu, P.G., Wu, C., Yates, J.R., 3rd, Su, A.I., Kelly, J.W., and Wiseman, R.L. (2013). Stress-independent activation of XBP1s and/or ATF6 reveals three functionally diverse ER proteostasis environments. Cell Rep. *3*, 1279–1292. https://doi.org/10.1016/j.celrep.2013.03.024.

100. Wu, J., Rutkowski, D.T., Dubois, M., Swathirajan, J., Saunders, T., Wang, J., Song, B., Yau, G.D.Y., and Kaufman, R.J. (2007). ATF6alpha optimizes long-term endoplasmic reticulum function to protect cells from chronic stress. Dev. Cell *13*, 351–364. https://doi.org/10.1016/j.devcel.2007.07.005.

101. Basheer, R., Rainnie, D.G., Porkka-Heiskanen, T., Ramesh, V., and McCarley, R.W. (2001). Adenosine, prolonged wakefulness, and A1-activated NF-kappaB DNA binding in the basal forebrain of the rat. Neuroscience *104*, 731–739. https://doi.org/10.1016/s0306-4522(01)00111-7.

102. Irwin, M.R., Wang, M., Ribeiro, D., Cho, H.J., Olmstead, R., Breen, E.C., Martinez-Maza, O., and Cole, S. (2008). Sleep loss activates cellular inflammatory signaling. Biol. Psychiatry *64*, 538–540. https://doi.org/10.1016/j.biopsych.2008.05.004.

103. Barcelos, R.P., Lima, F.D., Carvalho, N.R., Bresciani, G., and Royes, L.F. (2020). Caffeine effects on systemic metabolism, oxidative-inflammatory pathways, and exercise performance. Nutr. Res. *80*, 1–17. https://doi.org/10.1016/j.nutres.2020.05.005.

104. Giskeodegard, G.F., Davies, S.K., Revell, V.L., Keun, H., and Skene, D.J. (2015). Diurnal rhythms in the human urine metabolome during sleep and total sleep deprivation. Sci. Rep. *5*, 14843. https://doi.org/10.1038/srep14843.

105. Schmid, S.M., Hallschmid, M., Jauch-Chara, K., Wilms, B., Lehnert, H., Born, J., and Schultes, B. (2011). Disturbed glucoregulatory response to food intake after moderate sleep restriction. Sleep *34*, 371–377. https://doi.org/10.1093/sleep/34.3.371.

106. Broussard, J.L., Chapotot, F., Abraham, V., Day, A., Delebecque, F., Whitmore, H.R., and Tasali, E. (2015). Sleep restriction increases free fatty acids in healthy men. Diabetologia *58*, 791–798. https://doi.org/10.1007/s00125-015-3500-4.

107. Reynolds, A.C., Dorrian, J., Liu, P.Y., Van Dongen, H.P.A., Wittert, G.A., Harmer, L.J., and Banks, S. (2012). Impact of five nights of sleep restriction on glucose metabolism, leptin and testosterone in young adult men. PLoS One *7*, e41218. https://doi.org/10.1371/journal.pone.0041218.

108. Cappuccio, F.P., D'Elia, L., Strazzullo, P., and Miller, M.A. (2010). Sleep duration and all-cause mortality: a systematic review and meta-analysis of prospective studies. Sleep *33*, 585–592. https://doi.org/10.1093/sleep/33.5.585.

109. Shinohara, M., Tachibana, M., Kanekiyo, T., and Bu, G. (2017). Role of LRP1 in the pathogenesis of Alzheimer's disease: evidence from clinical and preclinical studies. J. Lipid Res. *58*, 1267–1281. https://doi.org/10.1194/jlr.R075796.

110. Kanekiyo, T., and Bu, G. (2014). The low-density lipoprotein receptor-related protein 1 and amyloid-beta clearance in Alzheimer's disease. Front. Aging Neurosci. *6*, 93. https://doi.org/10.3389/fnagi.2014.00093.

111. Lee, J., Lee, H., Lee, H., Shin, M., Shin, M.G., Seo, J., Lee, E.J., Park, S. A., and Park, S. (2023). ANKS1A regulates LDL receptor-related protein 1 (LRP1)-mediated cerebrovascular clearance in brain endothelial cells. Nat. Commun. *14*, 8463. https://doi.org/10.1038/s41467-023-44319-3.

112. Osgood, D., Miller, M.C., Messier, A.A., Gonzalez, L., and Silverberg, G. D. (2017). Aging alters mRNA expression of amyloid transporter genes at the blood-brain barrier. Neurobiol. Aging *57*, 178–185. https://doi.org/10.1016/j.neurobiolaging.2017.05.011.

113. He, S., Zhang, X., and Qu, S. (2019). Glutamate, Glutamate Transporters, and Circadian Rhythm Sleep Disorders in Neurodegenerative Diseases. ACS Chem. Neurosci. *10*, 175–181. https://doi.org/10.1021/acschemneuro.8b00419.

114. Sandhu, M.R.S., Dhaher, R., Gruenbaum, S.E., Raaisa, R., Spencer, D. D., Pavlova, M.K., Zaveri, H.P., and Eid, T. (2020). Circadian-Like Rhythmicity of Extracellular Brain Glutamate in Epilepsy. Front. Neurol. *11*, 398. https://doi.org/10.3389/fneur.2020.00398.

115. Videnovic, A., and Zee, P.C. (2015). Consequences of Circadian Disruption on Neurologic Health. Sleep Med. Clin. *10*, 469–480. https://doi.org/10.1016/j.jsmc.2015.08.004.

116. Chen, S.J., Deng, Y.T., Li, Y.Z., Zhang, Y.R., Zhang, W., Chen, S.D., Wu, B.S., Yang, L., Dong, Q., Feng, J., et al. (2022). Association of circadian rhythms with brain disorder incidents: a prospective cohort study of 72242 participants. Transl. Psychiatry *12*, 514. https://doi.org/10.1038/s41398-022-02278-1.

117. McEwen, B.S., and Karatsoreos, I.N. (2015). Sleep Deprivation and Circadian Disruption: Stress, Allostasis, and Allostatic Load. Sleep Med. Clin. *10*, 1–10. https://doi.org/10.1016/j.jsmc.2014.11.007.

118. Bruderer, R., Bernhardt, O.M., Gandhi, T., Miladinović, S.M., Cheng, L.Y., Messner, S., Ehrenberger, T., Zanotelli, V., Butscheid, Y., Escher, C., et al. (2015). Extending the limits of quantitative proteome profiling with data-independent acquisition and application to acetaminophen-treated three-dimensional liver microtissues. Mol. Cell. Proteomics *14*, 1400–1410. https://doi.org/10.1074/mcp.M114.044305.

119. Dobin, A., Davis, C.A., Schlesinger, F., Drenkow, J., Zaleski, C., Jha, S., Batut, P., Chaisson, M., and Gingeras, T.R. (2013). STAR: ultrafast universal RNA-seq aligner. Bioinformatics *29*, 15–21. https://doi.org/10.1093/bioinformatics/bts635.

120. Langmead, B., and Salzberg, S.L. (2012). Fast gapped-read alignment with Bowtie 2. Nat. Methods *9*, 357–359. https://doi.org/10.1038/nmeth.1923.

121. Robinson, J.T., Thorvaldsdóttir, H., Winckler, W., Guttman, M., Lander, E.S., Getz, G., and Mesirov, J.P. (2011). Integrative genomics viewer. Nat. Biotechnol. *29*, 24–26. https://doi.org/10.1038/nbt.1754.

122. Li, H., Handsaker, B., Wysoker, A., Fennell, T., Ruan, J., Homer, N., Marth, G., Abecasis, G., and Durbin, R.; 1000 Genome Project Data Processing Subgroup (2009). The Sequence Alignment/Map format and SAMtools. Bioinformatics *25*, 2078–2079. https://doi.org/10.1093/bioinformatics/btp352.

123. Ge, S.X., Son, E.W., and Yao, R. (2018). iDEP: an integrated web application for differential expression and pathway analysis of RNA-Seq data. BMC Bioinf. *19*, 534. https://doi.org/10.1186/s12859-018-2486-6.

124. Babicki, S., Arndt, D., Marcu, A., Liang, Y., Grant, J.R., Maciejewski, A., and Wishart, D.S. (2016). Heatmapper: web-enabled heat mapping for all. Nucleic Acids Res. *44*, W147–W153. https://doi.org/10.1093/nar/gkw419.

125. Kulak, N.A., Pichler, G., Paron, I., Nagaraj, N., and Mann, M. (2014). Minimal, encapsulated proteomic-sample processing applied to copy-number estimation in eukaryotic cells. Nat. Methods *11*, 319–324. https://doi.org/10.1038/nmeth.2834.

126. Meier, F., Brunner, A.D., Frank, M., Ha, A., Bludau, I., Voytik, E., Kaspar-Schoenefeld, S., Lubeck, M., Raether, O., Bache, N., et al. (2020). diaPASEF: parallel accumulation-serial fragmentation combined with data-independent acquisition. Nat. Methods *17*, 1229–1236. https://doi.org/10.1038/s41592-020-00998-0.

127. Livak, K.J., and Schmittgen, T.D. (2001). Analysis of relative gene expression data using real-time quantitative PCR and the 2(-Delta Delta C(T)) Method. Methods *25*, 402–408. https://doi.org/10.1006/meth.2001.1262.

STAR★METHODS

KEY RESOURCES TABLE

REAGENT or RESOURCE	SOURCE	IDENTIFIER
Antibodies		
Anti-PAX6 antibody [EPR15858], rabbit	Abcam	Cat#ab195045; RRID: AB_2750924
Hsc70/HSPA8 rabbit mAb	Abclonal	Cat#A0415; RRID: AB_2861461
Doublecortin/DCX antibody (E-6), mouse	Santa Cruz	Cat#sc-271390; RRID: AB_10610966
OLIG2 polyclonal antibody, rabbit	ProteinTech	Cat#13999-1-AP; RRID: AB_2157541
GFAP monoclonal antibody, clone 4B2E10, mouse	ProteinTech	Cat#60190-1-Ig; RRID: AB_10838694
anti-eIF2α antibody Subunit 1, rabbit	Abcam	Cat#ab137626; RRID: AB_2736873
Phospho-eIF2α (Ser51) antibody, rabbit	Cell Signaling Technology	Cat#9721; RRID: AB_330951
Recombinant anti-vinculin antibody [EPR8185], rabbit	Abcam	Cat#ab129002; RRID: AB_11144129
GAPDH polyclonal antibody, rabbit	ProteinTech	Cat#10494-1-AP; RRID: AB_2263076
anti-rabbit IgG, HRP-conjugated	R&D system	Cat#HAF008; RRID: AB_357235
anti-mouse IgG, HRP-linked	Cell Signaling Technology	Cat#7076S; RRID: AB_330924
Biological samples		
Human plasma from Adequate and restricted sleep	Shah et al.[54]	ClinicalTrials.gov NCT02835261
Chemicals, peptides, and recombinant proteins		
Matrigel®	Corning	Cat#354230
Accutase	Sigma	Cat#SCR005
PluriSTEM® medium	Sigma	Cat#SCM130
Rock inhibitor (Y27632)	Selleckchem	Cat#S1049
PSC neural induction medium	Gibco	Cat#A1647801
Neurobasal™ medium	Gibco	Cat#21103049
Advanced DMEM	Gibco	Cat#12491015
B-27™ serum-free supplement	Gibco	Cat#17504044
N-2 supplement	Gibco	Cat#17502048
GlutaMAX™-I supplement	Gibco	Cat#35050061
T3 (3,3′,5-Triiodo-L-thyronine sodium salt)	Sigma	Cat#T6397
Fetal Bovine Serum HI regular, USDA Approved Origin	Corning	Cat#35-011-CV
Dibutyryl cAMP	Sigma	Cat#D0627
Glutamic acid	Sigma	Cat#G5667-100G
Methionine	Sigma	Cat#M9625
NucBlue™ Live ReadyProbes™(Hoechst 33342)	Invitrogen	Cat#R37605
Live cell imaging solution	ThermoFisher Scientific	Cat#A14291DJ
GeneJET RNA purification kit	ThermoFisher Scientific	Cat#K0732
qScript™ XLT cDNA SuperMix	QuantaBio	Cat#95161-100
PowerUp™ SYBR™ green master mix	ThermoFisher Scientific	Cat#A25778
SYTOX™ red dead cell stain	ThermoFisher Scientific	Cat#S34859
RIPA lysis buffer	Boston BioProducts	Cat#NC9193720
Protease inhibitor cocktail	Sigma	Cat#P8340
Halt™ phosphatase inhibitor cocktail	Thermo Fisher Scientific	Cat#78428
1-Shot Digital-ECL substrate solution	Kindle biosciences	Cat#R1003

(*Continued on next page*)

Continued

REAGENT or RESOURCE	SOURCE	IDENTIFIER
CellTiter 96® non-radioactive cell proliferation assay (MTT) Kit	Promega	Cat#G4100
Critical commercial assays		
MxP® Quant 500 kit	Biocrates	Product#21094.12
High Select™ Top 14 Depletion Spin Columns	ThermoFisher Scientific	Cat#A36369
Deposited data		
Raw and analyzed RNA-seq data	This study	GEO: GSE254828
Metabolomics data	This study	Table S2
Proteomics data	This study	Table S4
ATF6 ChIP-seq in HepG2 cells	Encode project consortium[58]	GSM5214215 (https://www.encodeproject.org/ENCBS457OKW/)
ATF6 interactome	Encode project consortium[58]	https://www.encodeproject.org/ENCBS457OKW/
Human Transcription Factors annotation	Lambert et al.[57]	
Experimental models: Cell lines		
FUCCI-hESC	Singh et al.[77]	
FUCCI-NSCs	This Study	
Oligonucleotides		
GAPDH fwd	This Study	TCTGCTCCTCCTGTTCGACA
GAPDH rev	This Study	AAAAGCAGCCCTGGTGACC
hPOU5F1/Oct4 fwd	This Study	TCGAGAACCGAGTGAGAGGC
hPOU5F1/Oct4 rev	This Study	CACACTCGGACCACATCCTTC
NANOG fwd	This Study	CCAACATCCTGAACCTCAGCTAC
NANOG rev	This Study	GCCTTCTGCGTCACACCATT
NESTIN fwd	This Study	CAGGAGAAACAGGGCCTACA
NESTIN rev	This Study	TGGGAGCAAAGATCCAAGAC
PAX6 fwd	This Study	CTTTGCTTGGGAAATCCGAG
PAX6 rev	This Study	AGCCAGGTTGCGAAGAACTC
DCX fwd	This Study	TTCAAGGGGATTGTGTACGCT
DCX rev	This Study	GTCAGACAGAGATCGCGTCAG
OLIG2 fwd	This Study	CCAGAGCCCGATGACCTTTTT
OLIG2 rev	This Study	CACTGCCTCCTAGCTTGTCC
GFAP fwd	This Study	AGGTCCATGTGGAGCTTGAC
GFAP rev	This Study	GCCATTGCCTCATACTGCGT
Software and algorithms		
Biocrates MetIDQ™ software	Biocrates Life Sciences AG, Innsbruck, Austria	https://biocrates.com/webidq/
MetaboAnalyst v5.0	Peng et al.[75]	https://www.metaboanalyst.ca/
Perseus	Tyanova et al.[55]	https://maxquant.net/perseus/
Spectronaut Pulsar X	Bruderer, R. et al..[118]	https://biognosys.com/
CellProfiler v4.0.7	Stirling et al.[84]	www.cellprofiler.org
QuantStudio™ design and analysis software v1.5.1	Thermo Fisher Scientific	https://www.thermofisher.com/us/en/home/technical-resources/software-downloads/quantstudio-3-5-real-time-pcr-systems.html
FCS Express software	*De Novo* Software. (2025)	https://denovosoftware.com/
STAR v2.7.6a	Dobin A, Davis CA, Schlesinger F et al.[119]	https://github.com/alexdobin/STAR

(*Continued on next page*)

Continued

REAGENT or RESOURCE	SOURCE	IDENTIFIER
Cufflinks v2.2.1	Trapnell et al. 2010 https://doi.org/10.1038/nbt.1621	https://cole-trapnell-lab.github.io/cufflinks/
Bowtie2 v2.3.5	Langmead B et al.[120]	http://bowtie-bio.sourceforge.net/bowtie2/
IGV v2.10.2	Robinson J et al.[121]	https://software.broadinstitute.org/software/igv
Samtools v1.10	Li, H. et al.[122]	http://www.htslib.org/
iDEP v2.0	Ge, X. et al.[123]	https://bioinformatics.sdstate.edu/idep/
R-Studio v 2023.06.0	Integrated Development for R. RStudio, PBC, Boston, MA	https://cran.rstudio.com/
Morpheus	Broad Institute	https://software.broadinstitute.org/morpheus
Heat mapper	Babicki S et al.[124]	http://www.heatmapper.ca/expression/
Inkscape v0.92.4	Inkscape Project. (n.d.). *Inkscape*	https://inkscape.org/
Biorender		https://www.biorender.com/
Metascape	Zhou et al.[56]	https://metascape.org
Other		
Xevo TQS triple quadrupole mass spectrometer integrated with a Waters Acquity UHPLC	Waters	https://www.waters.com/nextgen/en.html
timsTOF Pro	Bruker	https://www.bruker.com/en/products-and-solutions/mass-spectrometry/timstof/timstof-pro-2.html
Celldiscoverer 7	Zeiss	https://www.zeiss.com/microscopy/us/products/imaging-systems/celldiscoverer-7.html
QuantStudio™ 5 real-time PCR system	ThermoFisher Scientific	Cat#A34322
Amersham ImageQuant 800	Cytiva	Product#29399481
SpectraMax iD3 microplate reader	Avantor	Cat#75886-128

EXPERIMENTAL MODEL AND STUDY PARTICIPANT DETAILS

Study participants, sleep restriction intervention, and plasma samples

The clinical trial details are provided here (ClinicalTrials.gov NCT02835261[53,54]). Briefly, study participants (healthy women, i.e., persons whose female sex was assigned at birth and hereafter referred to as women in the manuscript) with adequate habitual sleep duration (7-9 h/night confirmed objectively by a 2-week actigraphy screening) were randomly assigned to a 6-week adequate sleep phase or a 6-week sleep restriction phase followed by a 6-week washout period and crossover to the alternate sleep phase. The adequate sleep phase was defined as the duration of sleep between the regular bed and wake times of the participant determined during the actigraphy screening. The sleep restriction phase was defined as delaying bedtime by 1.5 hours while keeping the wake-up time unchanged. Participants remained blind to their randomization sequence until the beginning of the study. The duration of sleep was objectively assessed by actigraphy, a standard practice for the objective assessment of sleep duration in a free-living environment. Detailed exclusion criteria were previously published,[54] and continuous electroencephalogram (EEG) monitoring for six weeks per study phase (i.e., adequate vs. restricted sleep) was not feasible under the trial conditions. Briefly, participants were free of any medical, neurological, or psychiatric condition, eating or sleeping disorder, and regular use of any medications or supplements, including oral contraceptives. The Columbia University Institutional Review Board approved the study, and all participants gave written informed consent. Blood was collected only once between 10-11 am in fasting conditions after completion of each sleep phase, precluding assessment of changes in circadian rhythm. As previously reported, SR did not significantly affect weight, blood pressure, daytime physical activity, or plasma cortisol levels.[54] In the present study, we used blood plasma samples collected from healthy young women (n = 20) between 21 and 35 years of age to minimize age-related hormonal changes (Figure 1A).

Cell culture of FUCCI-hESCs

WA09 or H9 FUCCI-hESCs[77] were grown on Matrigel (Cat. No. 354230, Corning) coated plates using PluriSTEM medium (Cat. No. SCM130, Sigma). FUCCI-hESCs were passaged weekly using accutase (3-5 min, Cat. No. SCR005, Sigma) and seeded in PluriSTEM medium supplemented with rock inhibitor (Y27632, cat. no. S1049, Selleckchem) for better survival of single cell hESCs. All cells were cultured at 37°C with 5% CO_2.

Differentiation of FUCCI-hESCs to FUCCI-NSCs

Following the manufacturer's details, FUCCI-hESCs were differentiated into FUCCI-hNSCs using a commercially available PSC neural induction medium (Cat. No. A1647801, Gibco). Briefly, 250 $\times$ 10^3 FUCCI-hESCs were seeded in a 6-well plate in PluriSTEM medium supplemented with rock inhibitor. The next day, PluriStem medium was replaced with 2 ml of neural induction medium (49 ml of neurobasal medium + 1 ml of neural induction supplement) and cultured for 7 days with medium replacement every alternate day. After neural induction, cells were cultured and maintained in a neural expansion medium (49 ml neurobasal + 49 ml advanced DMEM + 2 ml neural induction supplement) with a medium change every alternate day and passaged using accutase (5-8 minutes) without rock inhibitor.

Differentiation of FUCCI-NSCs to neural, oligodendrocytes, and astrocytes

FUCCI-hNSCs (2.5 $\sim$ 5 $\times$ 10^4 cells/cm^2) were seeded on matrigel-coated plates in neural expansion medium (49 ml neurobasal + 49 ml advanced DMEM + 2 ml neural induction supplement). After two days, the medium was switched to neural differentiation medium (1x neurobasal medium, 2% B-27 serum-free supplement, and 2 mM GlutaMAX-I supplement) or oligodendrocyte differentiation medium (1x neurobasal medium, 2% B-27 serum-free supplement, 2 mM GlutaMAX-I, and 30 ng/mL T3 (Cat. No. T6397, Sigma)) or astrocyte differentiation medium (1x DMEM, 1% N-2 supplement, 2 mM GlutaMAX-I supplement, and 1% FBS). Although the manufacturers' protocol suggested changing the medium every 3-4 days, we changed the medium every other day for the metabolite treatment experiments. Of note, dibutyryl cAMP (0.5 mM, Sigma, Cat. No. D0627) was added from day 7 for a duration of 3 days for faster neural differentiation. The differentiation was carried out until days 9-10 before collecting the cells for qPCR and FACS experiments.

METHOD DETAILS

Targeted metabolomics and data analysis

The samples were prepared and analyzed using the commercially available MxP® Quant 500 kit (Biocrates Innsbruck, Austria; Figure S1A), strictly following their detailed protocol. The kit enables the quantification of up to 630 metabolites from 26 compound classes (e.g., amino acids, amino acids related, biogenic amines, bile acids, fatty acids, phosphatidylcholines, ceramides, di- and triglycerides). Lipids and hexoses were measured by flow injection analysis-tandem mass spectrometry (FIA-MS/MS), and small molecules were measured by liquid chromatography-tandem mass spectrometry (LC-MS/MS). The Q500 kit includes all the requisite seven calibration standards and three levels of QC samples. The experimental metabolomics measurement technique is described in detail by the patents EP1897014B1 and EP1875401B1. Briefly, a 96-well sample preparation device was used to analyze the metabolite profile in the samples quantitatively. This device consists of inserts impregnated with internal standards, and 10 μL of human plasma sample was added. Next, a phenyl isothiocyanate (PITC) solution was added to derivatize some of the analytes (e.g., amino acids). After derivatization, the target analytes were extracted with 5 mM ammonium acetate in methanol, followed by a dilution step. The extracts were then analyzed using FIA-MS/MS and LC-MS/MS methods, using multiple reaction monitoring (MRM) to detect the analytes. LCMS/MS analysis was performed using a platform comprising a Waters Xevo TQS triple quadrupole mass spectrometer integrated with a Waters Acquity UHPLC (Waters, Milford, MA). Concentrations were calculated using appropriate mass spectrometry software, and data were imported into Biocrates MetIDQ™ software for further analysis. Statistical data analysis was performed using MetaboAnalyst v5.0.[74–76] LoD (limit of detection) values smaller than the limits were converted to NA; metabolites with more than 20% missing values across samples were removed; remaining missing values were replaced with LoDs (1/5 of the minimum positive value for each metabolite). The data were logarithmically transformed prior to further analysis. Both fold-change analysis and partial least square discriminant analysis (PLS-DA) were performed to shortlist candidates based on the t-test and PLS-DA VIP (variable importance in projection) score, respectively. The joint pathway analysis feature of metaboanalyst v5.0[74–76] was used for GO analysis in Figure 3A using candidate proteins (n = 83; absolute difference > 0.2) and metabolites (n = 25, absolute $\log_2$ fold change >0.2, Table S7).

Proteomics and data analysis

Plasma samples were depleted for the top 14 high abundance plasma proteins using High Select Top 14 resin slurry (Cat. No. A36369, ThermoFisher Scientific). Briefly, 600 μL of High Select Top14 resin slurry was washed twice with 100 mM ammonium bicarbonate and mixed with 20 μL of neat plasma in a 96-well Agilent filter microplate. The microplate was incubated in a thermomixer at 450 rpm at room temperature for 30 min. The depleted plasma was then collected in a new 96-well collection plate under the filter plate by centrifugation at 100xg for 6 min. The depleted plasma samples were completely dried in a Speed-Vac vacuum concentrator without heat and resuspended in 11 μL of LC/MS grade water. Protein concentrations were determined using a BCA protein assay. Twenty (20) μg from each of these samples was resuspended in 20 μL of freshly prepared SDC lysis buffer (1% SDC, 10 mM TCEP, 40 mM CAA, and 100 mM Tris-HCl pH 8.5)[125] and boiled at 60°C for 20 min to denature, reduce and alkylate cysteines, followed by sonication in a water bath, cooled to room temperature. Protein digestion was processed in a 96-well plate overnight by adding LysC and trypsin in a 1:50 ratio (μg of enzyme to μg of protein) on a thermomixer at 37°C overnight at 500 rpm. The samples were acidified with 20% trifluoroacetic acid to a final concentration of 1%. The digested peptides were desalted using MacroSpin C18 in a 96-well plate format. The samples were dried in a Speed-Vac and resuspended in 10 μL of LC buffer (3% ACN/0.1% FA). Peptide

concentrations were determined using NanoDrop, and 200 ng of each sample was used to analyze PASEF and diaPASEF in timsTOF-Pro. Digested plasma samples were pooled and dried in Speed-Vac for spectral library generation, resuspended in 5% acetonitrile and 10 mM ammonium bicarbonate, pH 8.0, and subjected to BPRP (basic pH reversed-phase) chromatography. The fractions were collected in a 96-well plate and combined for a total of 24 fractions before desalting. The desalted peptides were dissolved in 10 μL of 3% acetonitrile/0.1% formic acid injected using PASEF. The peptides were separated within 90 min at a flow rate of 400 nL/min on a reversed-phase C18 column with an integrated CaptiveSpray Emitter (25 cm × 75 μm, 1.6 μm, IonOpticks). Mobile phases A and B were with 0.1% formic acid in water and 0.1% formic acid in ACN. The fraction of B was linearly increased from 2 to 25% within 60 min, followed by an increase to 35% within 10 min and a further increase to 80% before re-equilibration. The timsTOF Pro was operated in PASEF mode[126] with the following settings: Mass range 100 to 1700 m/z, 1/K0 Start 0.6 V·s/cm^{-2}, End 1.6 V·s/cm^{-2}, Ramp time 100 ms, Lock Duty Cycle to 100%, Capillary Voltage 1600V, Dry Gas 3 l/min, Dry Temp 200°C, PASEF settings: 10 MS/MS frames (1.16 seconds duty cycle), charge range 0-5, active exclusion for 0.4 min, Target intensity 20000, Intensity threshold 2500, CID collision energy 59eV. A polygon filter was applied to the *m/z* and ion mobility planes to select features most likely representing peptide precursors rather than singly charged background ions. The diaPASEF[126] experiment was acquired at defined 32 × 50 Th isolation windows from *m/z* 100 to 1,700. To adapt the MS1 cycle time in diaPASEF, the repetitions were set to 2 in the 16-scan diaPASEF scheme. The collision energy was ramped linearly as a function of the mobility from 59 eV at 1/K0 = 1.6 Vs cm^{-2} to 20 eV at 1/K0 = 0.6 Vs cm^{-2}. To generate the spectral libraries, we searched the acquired PASEF raw files and diaPASEF raw files with the Pulsar search engine using the hybrid spectral library generation functionality of Spectromine with default settings. The raw intensities for the proteins were calculated by summation of the peptide intensities. The diaPASEF data were analyzed with Spectronaut Pulsar X,[118] a software independent of the Mass Spectrometer vendor Biognosys. The default settings were used for the targeted analysis of DIA data in Spectronaut, except that the decoy generation was set to mutated. The false discovery rate (FDR) was estimated with the mProphet approach and set to 1% at the peptide precursor level and 1% at the protein level.

Metabolites treatment

To test the effect of metabolites on neuronal cells, FUCCI-hNSCs were seeded (2 × 10^3/well in a 96-well plate for short-term treatment or 10 × 10^3 in a 24-well plate for long-term treatment) with a neural expansion medium supplemented with 200 μM glutamic acid (Cat. No. G5667-100G, Sigma) or 35 μM methionine (Cat. No. M9625-25G, Sigma). Both metabolites at these concentrations were not toxic to cells (Figure S4B). Metabolites were replenished along with fresh medium every other day. Long-term treatment was carried out until day 30, with passaging every 4-6 days.

Live cell imaging and cell proliferation analysis pipeline

As mentioned above, FUCCI-hNSCs (2.5 to 5 × 10^3) were seeded per well of a 96-well plate and treated with metabolites. Cells were stained with NucBlue Live ReadyProbes (Hoechst 33342, Cat. No. R37605, Invitrogen) for 30 minutes, washed once with PBS, and imaged in live cell imaging solution (Cat. No. A14291DJ, ThermoFisher Scientific) using Celldiscoverer 7 (Zeiss). Cell counting was performed using CellProfiler software v4.0.7[84] with customized pipelines with the following settings Module 1: IdentifyPrimaryObjects: threshold strategy-Adaptive, Threshold method-Otsu, three classes thresholding, method to distinguish clumped objects-Intensity, method to draw dividing lines between clumped objects-Intensity; Module 2: OverlayOutlines; Module 3: SaveImages; and Module 4: ExportToSpreadsheet).

Quantitative real-time reverse transcription PCR

Cultured cells were washed once with PBS, and RNA was isolated using a GeneJET RNA purification kit (Cat. No. K0732, ThermoFisher Scientific) according to the manufacturer's instructions. cDNA synthesis was performed using qScript™ XLT cDNA SuperMix (Cat. No. 95161-100, QuantaBio). qRT-PCR reactions were performed using the QuantStudio™ 5 real-time PCR system (Cat. No. A34322, ThermoFisher Scientific) and PowerUp™ SYBR™ green master mix (Cat. No. A25778, ThermoFisher Scientific) in triplicate, with a template amount of 5-10 ng of cDNA for each reaction. The $\Delta\Delta C_T$ method[127] integrated into the QuantStudio™ design and analysis software v1.5.1 was used to analyze the fold change with *GAPDH* as the reference gene and FUCCI-hESCs as calibrator samples.

Flow cytometry

FUCCI-hESCs and hNSCs were dissociated with accutase, collected by centrifugation at 300 × *g* for 5 min, and kept on ice hereafter in polystyrene test tubes (Cat. No. 352058, Corning). Cells were resuspended in their respective medium, and 5 nM SYTOX™ red dead cell stain (Cat. No. S34859, ThermoFisher Scientific) was added directly to cells for dead cell exclusion and incubated for 20–25 min in the dark on ice. The unbound stains were washed once with 1 ml of cold PBS. Cells were passed through a cell-strainer cap on tubes (Cat. No. 352235, Corning) before analysis on the LSR II flow cytometer (BD Biosciences). Cell cycle analysis was performed using FCS Express software.

RNA-sequencing and data analysis

Total RNA from cultured cells was extracted using a GeneJET RNA purification kit (Cat. No. K0732) according to the manufacturer's protocol. RNA quality was evaluated by an Agilent 2100 BioAnalyzer. The preparation and sequencing of RNA-seq libraries were outsourced to BGI genomics. Libraries were sequenced on the NovaSeq 6000 platform with a 150-bp paired-end read length.

For RNA-seq data processing, reads were aligned to the human genome hg38 using STAR (v2.7.6a) with the default settings. Transcript assembly and differential expression analyses were performed using Cufflinks (v2.2.1). Assembly of novel transcripts was not allowed (-G). Other parameters of Cufflinks were the default setting. The summed FPKM (fragments per kilobase per million mapped reads) of transcripts sharing each gene ID was calculated and exported by the Cuffdiff program.

Downstream analysis was performed using iDEP (v1.1[123]) and R packages. GO analysis was performed using metascape.[56] Volcano plots, bar plots, and box plots were plotted using R software. Expression heatmaps were drawn using Morpheus (https://software.broadinstitute.org/morpheus) or heat mapper [124] online tools.

Western blotting

Whole-cell protein extracts were isolated from the cultured cells using RIPA lysis buffer (Boston BioProducts, Cat. No. NC9193720) supplemented with protease inhibitor cocktail (Sigma, Cat. No. P8340) and phosphatase inhibitor cocktail (Thermo Fisher Scientific, Cat. No. 78428). Blots were blocked using 5% skimmed milk powder/TBST at room temperature for 1-2 hours, and then they were incubated with the corresponding antibodies in 5% skimmed milk powder/TBST at 4°C overnight. Secondary antibodies were anti-rabbit IgG, HRP-linked antibody (1:5,000; R&D system, Cat. No. HAF008) and anti-mouse IgG, HRP-linked antibody (1:5,000; Cell Signaling Technology, Cat. No. 7076S), which were incubated for 1 hour at room temperature while shaking. The bands were developed using 1-Shot Digital-ECL substrate Solution (Kindle biosciences, Cat. No. R1003) and the blots were imaged using Amersham ImageQuant 800 (Cytiva).

Cell proliferation assay (MTT-based)

FUCCI-hNSCs were treated with glutamic acid or methionine for 26 days and then seeded into matrigel-coated microplates (tissue culture grade, 96 wells, flat bottom) at a density of 2×10^3 cells/well. The metabolites treatments were continued in microplates for 4 days with medium change every other day with fresh glutamic acid and methionine supplementation. On day 30, the MTT assay was performed using the CellTiter 96® non-radioactive cell proliferation assay (MTT) Kit (Promega, Cat. No. G4100), following the manufacturer's instructions. The absorbance was recorded at 570nm using a SpectraMax iD3 microplate reader.

Schematic representations

The illustrations in Figures 1A, 3B, 4A, 4C, 6A, 7, S1A, S2A, S3B, and S5G were drawn using Biorender (https://www.biorender.com).

QUANTIFICATION AND STATISTICAL ANALYSIS

The statistical analysis was performed with R (v4.1.0) scripts on the R-Studio platform (v2023.06.0). For metabolomic and proteomics data software in-built statistical analysis was followed in metaboanalyst[74–76] and perseus,[55] respectively. The box and violin plots in Figures S1D, 2D, S2C, 5C, and S5D, present the 25th, median, and 75th quartiles, and the whiskers extend 1.5 of interquartile ranges, and the *p*-value was calculated from the two-sided Mann-Whitney test. qPCR analysis was performed in technical triplicates, and the error bars indicate standard deviation of the mean. *p*-values were calculated using a two-sided T-test. A two-sided *p* less than 0.05 was considered statistically significant. All the detailed statistical analyses can be located in the corresponding method details and legend.

ADDITIONAL RESOURCES

Clinical trial registration and study details relevant to this paper are available at ClinicalTrials.gov under the identifier NCT02835261. This registry provides comprehensive information on the study design, recruitment status, and outcome measures. https://clinicaltrials.gov/ct2/show/NCT02835261.